DESY 16-061, KA-TP-14-2016, TTK-16-14

SusHi Bento: Beyond NNLO and the heavy-top limit

Robert V. Harlander[1], Stefan Liebler[2], Hendrik Mantler[3,4]

[1] *Institute for Theoretical Particle Physics and Cosmology*
RWTH Aachen University, 52056 Aachen, Germany
[2] *DESY, Notkestraße 85, 22607 Hamburg, Germany*
[3] *Institute for Theoretical Physics (ITP), Karlsruhe Institute of Technology*
Engesserstraße 7, 76128 Karlsruhe, Germany
[4] *Institute for Nuclear Physics (IKP), Karlsruhe Institute of Technology*
Hermann-von-Helmholtz-Platz 1, 76344 Eggenstein-Leopoldshafen, Germany

Abstract

Version `1.6.0` of the code `SusHi` is presented. Concerning inclusive CP-even Higgs production in gluon fusion, the following new features with respect to previous versions have been implemented: expansion of the partonic cross section in the soft limit, i.e. around $x = M_{\rm H}^2/\hat{s} \to 1$; N^{3}LO QCD corrections in terms of the soft expansion; top-quark mass suppressed terms through NNLO; matching to the cross section at $x \to 0$ through N^{3}LO. For CP-even and -odd scalars, an efficient evaluation of the renormalization-scale dependence is included, and effects of dimension-5 operators can be studied, which we demonstrate for the SM Higgs boson and for a CP-even scalar with a mass of 750 GeV. In addition, as a generalization of the previously available $b\bar{b} \to H$ cross section, `SusHi_1.6.0` provides the cross section for charged and neutral Higgs production in the annihilation of arbitrary heavy quarks. At fixed order in perturbation theory, `SusHi` thus allows to obtain Higgs cross-section predictions in different models to the highest precision known today. For the SM Higgs boson of $M_{\rm H} = 125\,\text{GeV}$, `SusHi` yields 48.28 pb for the gluon-fusion cross section at the LHC at 13 TeV. Simultaneously, `SusHi` provides the renormalization-scale uncertainty of $\pm 1.97\,\text{pb}$.

Email addresses: `robert.harlander@cern.ch` (Robert V. Harlander[1]), `stefan.liebler@desy.de` (Stefan Liebler[2]), `hendrik.mantler@kit.edu` (Hendrik Mantler[3,4])

1. Introduction

Since the year 2012, an important task of particle physics is to fully measure the properties of the Higgs boson with mass $M_{\rm H} \approx 125\,\text{GeV}$ discovered at the Large Hadron Collider (LHC) [1, 2]. At the same time, the search for additional Higgs bosons, which are predicted in many extended theories, is among the main missions of the LHC experiments. For this purpose, the knowledge of the corresponding production cross sections with high precision is of great relevance. The latest efforts in this direction are regularly summarized in the reports of the "LHC Higgs cross section working group" [3–6].

In this paper, we describe the new features that have been implemented in version `1.6.0` of the program `SusHi` [7, 8]. `SusHi` is a Fortran code which calculates Higgs-boson production cross sections through gluon fusion and bottom-quark annihilation in the Standard Model (SM), general Two-Higgs-Doublet Models (2HDM), the Minimal Supersymmetric Standard Model (MSSM) as well as its next-to-minimal extension (NMSSM), see Ref. [9].[1] Some of these additions to `SusHi` directly improve the theoretical predictions of the cross section; others are provided to allow for more sophisticated uncertainty estimates of these predictions. The new features are the following:

- `SusHi` now includes the next-to-next-to-next-to-leading order (N^3LO) terms for the gluon-fusion cross section of a CP-even Higgs boson in the heavy-top limit as described in Refs. [19–22].
- It provides the so-called soft expansion of the gluon-fusion cross section around the threshold of Higgs-boson production at $x \equiv M_\phi^2/\hat{s} = 1$, where $\hat{s}$ denotes the partonic center-of-mass energy and M_ϕ the Higgs-boson mass. This expansion is available for the cross sections in the heavy-top limit up to N^3LO for CP-even Higgs bosons. At next-to-leading order (NLO) and next-to-NLO (NNLO), the exact x-dependence is still available, of course, and remains the default.
- In addition, `SusHi_1.6.0` includes top-quark mass effects to the gluon-fusion cross section of a CP-even Higgs boson in the heavy-top limit up to NNLO, implemented through an expansion in inverse powers of the top-quark mass as described in Refs. [23–29]. The exact top-mass dependence at lowest order can be factored out. We remark that this feature is most interesting at NNLO, of course, since at leading order (LO) and NLO, `SusHi` also provides the full quark-mass dependence.
- A matching of the soft expansion to the high-energy limit [23–25], i.e. $x \to 0$, is available through N^3LO.
- The renormalization-scale dependence of the gluon-fusion cross section within an arbitrary interval is calculated in a single `SusHi` run.

[1] Other codes to obtain inclusive Higgs-boson cross sections through gluon fusion in the SM and beyond are described in Refs. [10–18].

- The effect of dimension-5 operators to the gluon-fusion cross section can be taken into account through N^{3}LO QCD for the inclusive cross section, and at LO and NLO (i.e. α_s^3) for the Higgs transverse momentum (p_T) distribution and (pseudo)rapidity distribution, respectively.
- Higgs-boson production cross sections through heavy-quark annihilation are implemented along the lines of Ref. [30], both for the NNLO QCD inclusive cross section, as well as for more exclusive cross sections up to NLO QCD.

All of the described features are applicable to Higgs-boson production in the theoretical models currently implemented in `SusHi`, even though some only work for low Higgs masses below the top-quark threshold $M_\phi < 2M_\mathrm{t}$ or for CP-even Higgs bosons.

Our paper is organized as follows: We start with a brief general overview of the code `SusHi` in Section 2, and subsequently present the new features implemented for the prediction of the gluon-fusion cross section in Section 3. This includes a theoretical description of the soft expansion, the inclusion of N^{3}LO terms and the top-quark mass effects in Sections 3.1–3.3. We proceed with a description of the "RGE procedure" to determine the renormalization-scale dependence of the gluon-fusion cross section in Section 3.4, and finally describe the implementation of an effective Lagrangian including dimension-5 operators in Section 3.5. The implementation of heavy-quark annihilation cross sections is described in Section 4. Numerical results are presented in Section 5; they also include a comparison of our results with the most recent literature.

2. The program `SusHi`

`SusHi` is a program originally designed to describe Higgs production in gluon fusion and bottom-quark annihilation in the MSSM. It collects a number of results from the literature valid through N^{3}LO in the strong coupling constant, and combines them in a consistent way. We subsequently discuss the present theoretical knowledge of the calculation of the gluon fusion and bottom-quark annihilation cross sections and their inclusion in `SusHi`.

It is well-known that QCD corrections to the gluon-fusion process $gg \to \phi$ [31], mediated through heavy quarks in the SM, are very large. NLO QCD corrections are known for general quark masses [32–37]. In the heavy-top limit, an effective theory can be constructed by integrating out the top quark. In this case, NNLO corrections have been calculated a long time ago [38–40]. The N^{3}LO contributions were only recently obtained in Refs. [19, 20, 22, 41, 42], while various parts of the N^{3}LO calculation have been calculated independently [21, 43–56]. Approximate N^{3}LO results were presented in Refs. [16, 17, 57]. Effects of a finite top-quark mass at NNLO were approximately taken into account in Refs. [23–29].

Many of these effects can be taken into account in the latest version of `SusHi`; this will be discussed in detail in Section 3. Electroweak corrections [58–60] can be included as well, either in terms of the full SM electroweak correction factor, or restricted to the corrections mediated by light quarks, the latter being a more conservative estimate in certain BSM

scenarios. For completeness, we note that effects beyond fixed order have been addressed through soft-gluon resummation [18, 61–67], but those are not included in SusHi.

If requested in the input file, SusHi uses the SM results described above also for the 2HDM, the MSSM or the NMSSM through the proper rescaling of the Yukawa couplings. In supersymmetric models, also squarks induce an interaction of the Higgs boson to two gluons. In the MSSM, the corresponding NLO virtual contributions, involving squarks, quarks and gluinos, are either known in an expansion of inverse powers of heavy SUSY masses [68–70] or in the limit of a vanishing Higgs mass, see Refs. [71–74]. In this limit, even NNLO corrections of stop-induced contributions are known, see Refs. [75, 76]; an approximation of these effects [77] is included in SusHi, see Ref. [78]. Whereas for the MSSM SusHi relies on both expansions, for the NMSSM the NLO virtual corrections are purely based on an expansion in heavy SUSY masses [9]. We note that numerical results for the exact NLO virtual contributions involving squarks, quarks, and gluinos were presented in Refs. [79, 80], and analytic results for the pure squark-induced contributions can be found in Refs. [36, 37, 81].

The associated production of a Higgs boson with bottom quarks, $pp \to b\bar{b}\phi$, is of particular relevance for Higgs bosons, where the Yukawa coupling to bottom quarks is enhanced. This happens in models with two Higgs doublets, for example, if $\tan\beta$, the ratio of the vacuum expectation values of the two neutral Higgs fields, is large. SusHi includes the cross section for this process in the so-called 5-flavor scheme, i.e. for the annihilation process $b\bar{b} \to \phi$. The inclusive cross section for this process is implemented at NNLO QCD [82, 83]; it is reweighted by effective Yukawa couplings in the model under consideration. SusHi_1.6.0 now also includes general heavy-quark annihilation cross sections [30] at NNLO QCD, which we will describe in Section 4.

For completeness we note that SusHi can be linked to FeynHiggs [84–87] and 2HDMC [88] to obtain consistent sets of parameters in the MSSM or the 2HDM, respectively.

SusHi is controlled via an SLHA-style [89] input file. In the following, we will refer to the entries of a Block "NAME" and their possible values as NAME(ENTRY)=VALUE. If more than one value is required, we write NAME(ENTRY)={VALUE1,VALUE2,...} or, when referring only to one specific value, NAME(ENTRY,1)=VALUE1, etc.

3. Higgs production through gluon fusion

The hadronic cross section for Higgs production in gluon fusion can be written as

$$\sigma(pp \to H + X) = \sum_{i,j\in\{q,\bar{q},g\}} \tilde{\phi}_i \otimes \tilde{\phi}_j \otimes \hat{\sigma}_{ij}\,, \tag{1}$$

where $\phi_i(x,\mu_\mathrm{F}) = \tilde{\phi}_i(x,\mu_\mathrm{F})/x$ are parton densities, q ($\bar{q}$) denotes the set of all (anti-)quarks ($q = t$ and $\bar{q} = \bar{t}$ can be neglected), and $\otimes$ is the convolution defined as

$$(f \otimes g)(z) \equiv \int_0^1 \mathrm{d}x_1 \int_0^1 \mathrm{d}x_2 f(x_1) g(x_2) \delta(z - x_1 x_2)\,. \tag{2}$$

The perturbative expansion of the partonic cross section,

$$\hat{\sigma}_{ij,\mathrm{N^nLO}} = \sum_{l=0}^{n} \hat{\sigma}_{ij}^{(l)} \,, \tag{3}$$

can be represented in terms of Feynman diagrams where the external partons couple to the Higgs bosons through a top-, bottom-, or charm-quark loop (contributions from lighter quarks are negligible).

The first two terms in the perturbative expansion of $\hat{\sigma}_{ij}$ ($l = 0, 1$ in Eq. (3)) are known for general quark mass and included in `SusHi_1.6.0`. The NNLO term $\hat{\sigma}_{ij}^{(2)}$ has been evaluated on the basis of an effective Higgs-gluon interaction vertex which results from integrating out the top quark from the SM Lagrangian. At NLO, it has been checked that this results in an excellent approximation of the NLO QCD correction factor to the LO cross section, even for rather large Higgs-boson masses. At NNLO, the validity of the heavy-top limit for the QCD corrections factor was investigated through the calculation of a number of terms in an expansion around $M_\mathrm{t}^2 \gg \hat{s}, M_\phi^2$, and matching it to the high-energy limit of $\hat{\sigma}_{ij}^{(2)}$ [23–29]. It was found that the mass effects to the QCD correction factor are at the sub-percent level.

Recently, also the N^{3}LO-term $\hat{\sigma}_{ij}^{(0)}$ has become available in terms of a soft expansion. We will comment on its implementation in the latest release of `SusHi` in Section 3.2.

The exact NLO and the approximate higher order results for the cross section are combined in `SusHi` through the formula

$$\sigma_\mathrm{X} = \sigma_\mathrm{NLO} + \Delta_\mathrm{X}\sigma^t \,, \qquad \Delta_\mathrm{X}\sigma^t \equiv (1+\delta_\mathrm{EW})\sigma_\mathrm{X}^t - \sigma_\mathrm{NLO}^t \,, \tag{4}$$

where σ_NLO refers to the NLO cross section with exact top-, bottom- and charm-mass dependence, while σ_X^t (X=N^{n}LO, $n \geq 1$) is obtained in the limit of a large top-quark mass. Electroweak effects [58], encoded in δ_EW, are included by assuming their full factorization from the QCD effects, as suggested by Ref. [90] for a SM Higgs boson. In BSM scenarios, this assumption may be no longer justified. `SusHi` therefore provides an alternative way to include electroweak effects which is based solely on the light-quark contributions to the electroweak correction factor; for details, we refer the reader to Refs. [7, 78]. For our purpose, it suffices to assume Eq. (4). The new release of `SusHi` provides various approximations to evaluate σ_X^t, in particular through expansions in $1/M_\mathrm{t}$, and expansions around $\hat{s} = M_\phi^2$.

In addition to σ_X, which can be found in `Block SUSHIggh`, `SusHi` also outputs the individual terms of Eq. (4). The exact LO and NLO cross sections are collected in `Block XSGGH`, while the σ_X^t are given in `Block XSGGHEFF`, which also contains the electroweak correction term δ_EW, if requested.

It is understood that the N^{n}LO terms in Eq. (4) are evaluated with N^{n}LO PDFs.[2] Note that this means that, for example, $\Delta_\mathrm{NNLO}\sigma^t$ is not simply the convolution of $\hat{\sigma}^{t,(2)}$ with NNLO

[2]Since N^{3}LO PDFs are not yet available, we use NNLO PDFs for the evaluation of the N^{3}LO cross section in this paper. The user of `SusHi` can specify the PDF set at each order individually.

PDFs, but retains a sensitivity to $\hat{\sigma}^{t,(1)}$. Thus, the final result for the NNLO gluon-fusion cross section obtained from `SusHi` through Eq. (4) depends on the approximation applied to the evaluation of both $\hat{\sigma}^{t,(2)}$ and $\hat{\sigma}^{t,(1)}$. If electroweak effects are included, this even holds for `SusHi`'s final result for σ_{NLO} due to the definition of $\Delta_{\text{X}}\sigma^t$ in Eq. (4).

In the remainder of this section, we first discuss the soft expansion around the threshold of Higgs production, $\hat{s} = M_\phi^2$, in Section 3.1. The implementation of N^{3}LO contributions is described in Section 3.2, and top-quark mass effects through NNLO as well as the matching to the high-energy limit in Section 3.3. While these features are only available for CP-even Higgs bosons (partially in a certain range of Higgs-boson masses M_ϕ only), the analytic calculation of the μ_{R} dependence of the gluon-fusion cross section described in Section 3.4 is available for all Higgs bosons. The inclusion of dimension-5 operators is discussed in Section 3.5.

3.1. Soft expansion

The NLO and NNLO coefficients of σ^t are approximated very well by the first few terms[3] in an expansion around the "soft limit", $x \to 1$. In fact, the gain of the full $\hat{s}$-dependence becomes doubtful anyway when working in the heavy-top limit, since the latter formally breaks down for $\hat{s} > 4M_{\text{t}}^2$, meaning $x \lesssim 0.13$ for $M_{\text{H}} = 125\,\text{GeV}$. Apart from the exact $\hat{s}$-dependence at LO, NLO, and NNLO, `SusHi_1.6.0` provides the soft expansion of the cross section for CP-even Higgs production through order $(1-x)^{16}$ at these perturbative orders, and also at N^{3}LO (for more details on the latter, see Section 3.2).

The precise way in which the soft expansion is applied is governed by the new `Block GGHSOFT`. Each line in this block contains four integers:

```
Block GGHSOFT
  <entry> <n1> <n2> <n3>
```

Following Section 2, we will refer to such a line as `GGHSOFT(<entry>)={<n1>,<n2>,<n3>}` in the text, and to the individual entries as `GGHSOFT(<entry>,1)=<n1>`, etc. Setting `GGHSOFT(`n`)={1,`N, a`}` evaluates the soft expansion of $\hat{\sigma}_{ij}^{t,(n)}$ in the following way:

$$\hat{\sigma}_{ij}^t \to \hat{\sigma}_{ij,N}^t \equiv x^a \mathcal{T}_N^x \left(\frac{\Delta\hat{\sigma}_{ij}^t}{x^a} \right) , \tag{5}$$

where $\mathcal{T}_N^x$ denotes the asymptotic expansion around $x = 1$ through order $(1-x)^N$, and a is a positive integer. Setting `GGHSOFT(`n`,2)=-1` will keep only the soft and collinear terms, whose x dependence is given by

$$\delta(1-x) \quad \text{or} \quad \left(\frac{\ln^k(1-x)}{1-x} \right)_+ , \quad k \geq 0 \tag{6}$$

[3]The first 16 terms in this expansion lead to an accuracy of better than 1% with respect to the heavy-top limit with exact x-dependence at NNLO, for example. For more details see below.

by definition. Here $(\cdot)_+$ denotes the usual plus distribution, defined by

$$\int_z^1 \mathrm{d}x \, (f(1-x))_+ \, g(x) = \int_z^1 \mathrm{d}x f(x) \, [g(x) - g(1)] + g(1) \int_0^z \mathrm{d}x f(x) \, . \tag{7}$$

The parameters `GGHSOFT(`n`)` apply to all partonic subchannels at order N^{n}LO, and to all terms in the $1/M_\mathrm{t}$ expansion as requested by the input `Block GGHMT`, see Section 3.3 below.

The exact x-dependence is obtained by setting `GGHSOFT(`n`,1)=0` (only available for $n \leq 2$). The other two entries in `GGHSOFT(`n`)` are then irrelevant. The default values for the block `GGHSOFT` through NLO are

default: `GGHSOFT(1,1)=0; GGHSOFT(2,1)=0; GGHSOFT(3)={1,16,0}.` (8)

Again, all terms of the soft expansion are available including the full μ_F- and μ_R-dependence.

A sample input block reads

```
Block GGHSOFT
  1 0 0 0
  2 1 16 1
  3 1 16 1
```

which provides the result including the exact x-dependence at NLO, and the soft expansion through $(1-x)^{16}$ at NNLO and N^{3}LO after factoring out a factor of x ($a = 1$ in Eq. (5)). We recall that these settings only affect the heavy-top results $\hat{\sigma}^t_\mathrm{X}$ in Eq. (4); σ_NLO is always calculated by taking into account the full quark-mass and x-dependence. The soft expansion is available for all CP-even Higgs bosons of arbitrary masses.

3.2. N^{3}LO terms

Recently, the N^{3}LO QCD corrections to the Higgs production cross section through gluon fusion have become available [19–22]. More specifically, the result was provided in terms of the soft expansion through order $(1-x)^{37}$ of the leading term in $1/M_\mathrm{t}$ for $\mu = \mu_\mathrm{R} = \mu_\mathrm{F}$. We implemented this expansion through $(1-x)^{16}$; higher order terms do not change the result within the associated uncertainty. In addition, we included the μ_F- and μ_R-dependent terms at the same order. Experience from NNLO lets one expect that these terms are sufficient to obtain an excellent approximation of the QCD correction factor to the LO cross section, at least for Higgs masses in the validity range of the effective theory description.

The N^{3}LO result is accessible in `SusHi_1.6.0` by setting the input parameter `SUSHI(5)=3`. This will evolve $\alpha_s(M_Z)$ to $\alpha_s(\mu_\mathrm{R})$ at 4-loop order when calculating the cross section, where μ_R/M_ϕ is defined in `SCALES(1)`. Note that with this setting, the hadronic cross section will formally still suffer from an inconsistency because N^{3}LO PDF sets are not yet available. As described in Section 3.1, the depth of the soft expansion at N^{3}LO, as well as the power a in Eq. (5) can be controlled through the input variables `GGHSOFT(3)`.[4]

[4]The setting `GGHSOFT(3,1)=0` is not available, of course.

Finally, we remark that, also at N^{3}LO, the full μ_R- and μ_F-dependence is available, again accessible through the variables `SCALES(1)` and `SCALES(2)`, respectively. It follows from invariance of the hadronic result under these scales, and only requires the NNLO result as input, as well as the QCD β function and the QCD splitting functions through three loops. The required convolutions can be evaluated with the help of the program `MT.m` [91], for example.

3.3. Top-quark mass effects

In versions before `SusHi_1.6.0`, only the formally leading terms in $1/M_t$ were available for $\hat{\sigma}_{ij}^{t,(2)}$. However, in order to allow for thorough studies of the theoretical uncertainty associated with the gluon-fusion cross section, `SusHi_1.6.0` includes also subleading terms in $1/M_t$ for the production of a CP-even Higgs (`SUSHI(2)`$\in$ {`11,12,13`}). There are a number of options provided by `SusHi_1.6.0` associated with this; they are controlled by the new input `Block GGHMT`.

First of all, `GGHMT(`n`)=`$P \in$ {`0,1,`$\ldots, P_n^{\max}$}` provides the expansion of $\hat{\sigma}_{ij}^{t,(n)}$ through $1/M_t^P$ (note that terms with odd $P$ vanish). In addition (or alternatively), one may define the depth of the expansion individually for each partonic channel $\hat{\sigma}_{ij}^{t,(n)}$ through the parameters `GGHMT(`$nm$`)=`$P \in$ {`0,1,`$\ldots, P_n^{\max}$}, where $ij = (gg, qg, q\bar{q}, qq, qq')$ corresponds to $m = (1, 2, 3, 4, 5)$, respectively. Currently, the maximal available depths of expansion are[5] $P_0^{\max} = P_1^{\max} = 10$ and $P_2^{\max} = 6$.

The default settings are

default: `GGHMT(0)=-1 ; GGHMT(1)=0 ; GGHMT(2)=0 ;`
`GGHMT(1`i`)=GGHMT(1)` , $i = 1, \ldots, 3$; `GGHMT(2`i`)=GGHMT(2)` , $i = 1, \ldots, 5$, (9)

where `GGHMT(0)=-1` means to keep the full top mass dependence. Let us recall that these settings only affect the heavy-top results $\hat{\sigma}_X^t$ in Eq. (4); σ_{NLO} is always calculated by taking into account the full quark-mass dependence.

As an example, consider the input

```
Block GGHMT
  1    10
  13   0
  2    6
  23   0
  24   0
  25   0
```

which will cause `SusHi_1.6.0` to

- keep the full top mass dependence at LO
- expand the NLO terms $\hat{\sigma}_{gg}^{t,(1)}$ and $\hat{\sigma}_{qg}^{t,(1)}$ through $1/M_t^{10}$

[5] For the $q\bar{q}$-channel, the maximum reduces to $P_2^{\max} = 4$, if a soft expansion beyond $N = 13$ is requested.

- expand the NNLO terms $\hat{\sigma}_{gg}^{t,(2)}$ and $\hat{\sigma}_{qg}^{t,(2)}$ through $1/M_\mathrm{t}^6$
- keep only the terms of order $1/M_\mathrm{t}^0$ for the pure quark channels at NLO and NNLO.

This also shows that the variables `GGHMT(`nm`)` overrule the setting of `GGHMT(`n`)` for the individual channels. This may be desirable as it is known that the pure quark channels show a rather bad convergence behavior [24–29], so one may want to include only a small number of terms for them in the $1/M_\mathrm{t}$ expansion. By convention, `GGHMT(`n`)` must always be at least as large as the maximum of `GGHMT(`nm`)`; if this is not the case in the input file, `SusHi` will override the user's definition of `GGHMT(`n`)` and set it to the maximum of all `GGHMT(`nm`)`.

In the strict heavy-top limit (i.e., $P = 0$), the quality of the approximation improves considerably if one factors out the LO mass dependence σ_0^t [34, 92] before the expansion, given by

$$\sigma_0^t = \frac{\pi\sqrt{2}G_\mathrm{F}}{256}\left(\frac{\alpha_s}{\pi}\right)^2\tau^2\left|1+(1-\tau)\arcsin^2\frac{1}{\sqrt{\tau}}\right|^2, \qquad \tau = \frac{4M_\mathrm{t}^2}{M_\phi^2}, \tag{10}$$

where $G_\mathrm{F} \approx 1.16637\cdot 10^{-5}\,\mathrm{GeV}^{-2}$ [93] is Fermi's constant. The generalization to higher orders in $1/M_\mathrm{t}$ corresponds to

$$\hat{\sigma}_{ij}^{t,(n)} = \sigma_0^t\frac{\mathcal{T}_{P_{n,ij}}\hat{\sigma}_{ij}^{t,(n)}}{\mathcal{T}_{P_n}\sigma_0^t}, \tag{11}$$

where $\mathcal{T}_P$ denotes an operator that performs an asymptotic expansion through order $1/M_\mathrm{t}^P$. In a strict sense, it should be $P_n = P_{n,ij}$; however, `SusHi` allows only for a global value of P_n here, which applies to all sub-channels ij and is set to `GGHMT(`n`)`.

Setting `GGHMT(-1)=`n factors out the LO mass dependence through order n, i.e.

$$\hat{\sigma}_{ij}^t = \sigma_0^t\sum_{k=0}^{n}\frac{\mathcal{T}_{P_{k,ij}}\hat{\sigma}_{ij}^{t,(k)}}{\mathcal{T}_{P_k}\sigma_0^t} + \sum_{k\geq n+1}\mathcal{T}_{P_{k,ij}}\hat{\sigma}_{ij}^{t,(k)}. \tag{12}$$

This will affect all partonic channels. The default setting is

$$\boxed{\textit{default:}}\quad \texttt{GGHMT(-1)=3} \tag{13}$$

which means that the LO M_t dependence is factored out from all available orders.

It was observed that higher orders in $1/M_\mathrm{t}$ in general spoil the validity of the expansion, since its radius of convergence is formally restricted to $\hat{s} < 4M_\mathrm{t}^2$. This manifests itself in the expansion coefficients containing positive powers of $\hat{s}/M_\phi^2$. In order to tame the corresponding divergence as $\hat{s}\to\infty$, it was suggested to match the result to the asymptotic behavior in this limit, which is known from Refs. [23, 24]. Whether or not such a matching is performed for $\hat{\sigma}_{ij}^{t,(n)}$ is governed by the parameter `GGHMT(`$n\cdot$`10)` (i.e. `GGHMT(10)`, `GGHMT(20)`, ...). By default,

$$\boxed{\textit{default:}}\quad \texttt{GGHMT(}n\cdot\texttt{10)=0}\,,\ n=1,\ldots,3\,, \tag{14}$$

meaning that no matching is done; setting `GGHMT(`n`·10)=1` switches the matching on for all partonic subchannels at order N^{n}LO.

As we will find in Section 5, the matching to $x \to 0$ is helpful in approximating the full cross section even at $1/M_\mathrm{t}^0$. Thus, we provide the possibility to do this matching also at N^{3}LO, even though top-mass suppressed terms are not yet known at this order. The form of the matching through NNLO has been introduced in Refs. [24, 25]; here we adopt the same strategy, generalized to N^{3}LO:

$$\begin{aligned}\hat{\sigma}_{ij}^{t,(n)}(x) = \hat{\sigma}_{ij,N}^{t,(n)}(x) + \sigma_0^t \sum_{l=1}^{n-1} A_{ij}^{(n,l)} \left[\ln\frac{1}{x} - \sum_{k=1}^{N}\frac{1}{k}(1-x)^k\right]^l \\ + (1-x)^{N+1}\left[\sigma_0^t B_{ij}^{(n)} - \hat{\sigma}_{ij,N}^{t,(n)}(0)\right],\end{aligned} \tag{15}$$

where $\sigma_0^t B_{ij}^{(0)} = \hat{\sigma}_{ij,N}^{t,(0)}(0) = 0$, and $\hat{\sigma}_{ij,N}^{t,(n)}(x)$ denotes the soft expansion of the cross section through order $(1-x)^N$, see Eq. (5). The coefficients $B_{ij}^{(1)}$ and $A_{ij}^{(2,1)}$ are given in numerical form in Refs. [23, 24, 94],[6] while $A_{gg}^{(3,2)}$ can be found in Ref. [94] (where it is called $C_\mathrm{A}^3\mathcal{C}^{(3)}$). For the unknown coefficients through N^{3}LO, *we assume*

$$\sigma_0^t B_{ij}^{(n)} = \hat{\sigma}_{ij,N}^{t,(n)}(0) \quad \text{for} \quad n \geq 2\,, \qquad A_{ij}^{(3,1)} = 0\,. \tag{16}$$

The technical consequence of the matching procedure implemented in `SusHi` is that it *requires* the cross section to be expressed in terms of the soft expansion, i.e., one needs to set `GGHSOFT(`n`,1)=1` if the N^{n}LO cross section is requested.

The effect of the matching at N^{3}LO is shown in Fig. 1: the soft expansion tends to a constant towards $x \to 0$ by construction, and cannot reproduce the $\ln^2 x$-behavior of the exact result. The merging of the two limits is very smooth and suggests that the matched curve is not too far from the full result. Of course, the fact that some coefficients in Eq. (15) are unknown introduces a theoretical uncertainty. However, we observe a change in the final cross section of only about 0.5% when setting $A_{gg}^{(3,1)} = A_{gg}^{(3,2)}$ for a SM Higgs, for example.

It remains to say that all terms in $1/M_\mathrm{t}$ are available including the full μ_F- and μ_R-dependence. As in earlier versions of `SusHi`, these parameters are accessible through the input parameters `SCALES(1)` and `SCALES(2)`. Since top-quark mass effects are not known for the N^{3}LO cross section, all settings of `GGHMT` involving $n = 3$ except from `GGHMT(30)` have no effect in the current version `SusHi_1.6.0`. The inclusion of $1/M_\mathrm{t}$ terms is only available for $M_\phi < 2M_\mathrm{t}$ and the matching to the high-energy limit only in a mass range $M_\phi \in [100\,\mathrm{GeV}, 300\,\mathrm{GeV}]$.

[6] The notation for $A_{ij}^{(2,1)}$ is $A_{ij}^{(2)}$ in that paper.

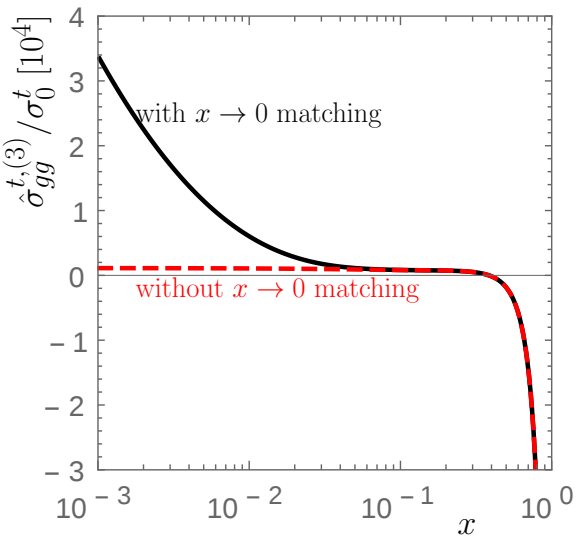

Figure 1: Partonic cross section $\hat{\sigma}_{gg}^{t,(3)}/\sigma_0^t$ in 10^4 according to Eq. (15) as a function of $x = M_\phi^2/\hat{s}$ with and without matching to the high-energy limit. The order of the soft expansion applied in both cases is $(1-x)^{16}$.

3.4. Renormalization scale dependence

The renormalization scale (μ_R) dependence of the partonic cross section can be written as

$$\hat{\sigma}_{ij} = \sum_{n\geq 0} \sum_{l=0}^{n} \left(\frac{\alpha_s(\mu_\mathrm{R})}{\pi}\right)^{n+2} \hat{\kappa}_{ij}^{(n,l)}(\mu_0)\, l_{\mathrm{R}0}^l\,, \tag{17}$$

where $l_{\mathrm{R}0} = 2\,\ln(\mu_\mathrm{R}/\mu_0)$, and μ_0 is an arbitrary reference scale. The coefficients $\hat{\kappa}_{ij}^{(n,l)}(\mu_0)$ are explicitly contained in `SusHi` (for $\mu_0 = M_\phi$). The dependence of the cross section on μ_R can be studied with `SusHi` by varying the input parameter `SCALES(1)`, which contains the numerical value for μ_R/M_ϕ. `SusHi` will then insert this value into Eq. (17) and convolve the resulting partonic cross section over the PDFs. A decent picture of the μ_R dependence may require to perform this "standard procedure" ten times or more.

`SusHi_1.6.0` provides a considerably faster way to obtain the μ_R dependence of the cross section by convolving the $\hat{\kappa}_{ij}^{(n,l)}(\mu_0)$ with the PDFs *before* varying μ_R,

$$\kappa^{(n,l)}(\mu_0) = \hat{\kappa}_{ij}^{(n,l)}(\mu_0) \otimes \tilde{\phi}_i \otimes \tilde{\phi}_j\,. \tag{18}$$

We will refer to this as the "RGE procedure". Due to the renormalization group equation[7]

$$\frac{\mathrm{d}}{\mathrm{d}\mu_\mathrm{R}^2}\sigma_{\mathrm{N}^n\mathrm{LO}} = \mathcal{O}(\alpha_s^{n+3}) = \frac{\mathrm{d}}{\mathrm{d}\mu_\mathrm{R}^2}\hat{\sigma}_{ij,\mathrm{N}^n\mathrm{LO}}\,, \tag{19}$$

[7]The power $n+3$ takes into account the fact that the LO cross section is of order α_s^2.

which holds both at the partonic and the hadronic level, it suffices to calculate the coefficients $\kappa^{(n,l)}(\mu_0)$ for $l = 0$ and $n \leq 2$ if the N^{3}LO result is requested. `SusHi_1.6.0` does this by initially assuming $\mu_0/M_\phi = \mu_\mathrm{R}/M_\phi =$ `SCALES(1)` in Eq. (17). All other coefficients are then determined via the QCD β function, defined through

$$\frac{\mathrm{d}}{\mathrm{d}\mu_\mathrm{R}^2}\alpha_s(\mu_\mathrm{R}) = \alpha_s(\mu_\mathrm{R})\beta(\alpha_s)\,, \qquad \beta(\alpha_s) = -\frac{\alpha_s}{\pi}\sum_{n\geq 0}\left(\frac{\alpha_s}{\pi}\right)^n \beta_n\,. \tag{20}$$

Explicitly, one finds

$$\begin{aligned}
&\kappa^{(1,1)} = 2\,\beta_0\,\kappa^{(0,0)}\,, \qquad \kappa^{(2,2)} = \frac{3}{2}\,\beta_0\,\kappa^{(1,1)}\,, \qquad \kappa^{(2,1)} = 2\,\beta_1\,\kappa^{(0,0)} + 3\,\beta_0\,\kappa^{(1,0)}\,,\\
&\kappa^{(3,3)} = \frac{4}{3}\beta_0\,\kappa^{(2,2)}\,, \qquad \kappa^{(3,2)} = \frac{3}{2}\,\beta_1\,\kappa^{(1,1)} + 2\,\beta_0\,\kappa^{(2,1)}\,,\\
&\kappa^{(3,1)} = 2\,\beta_2\,\kappa^{(0,0)} + 3\,\beta_1\,\kappa^{(1,0)} + 4\,\beta_0\,\kappa^{(2,0)}\,.
\end{aligned} \tag{21}$$

Inserting these coefficients into the hadronic analogue of Eq. (17), it is possible to obtain the hadronic cross section at any value of μ_R without any further numerical integration. Since the μ_R dependence is typically much larger than the μ_F dependence for gluon fusion, this feature of `SusHi` saves a significant amount of computing time when aiming for an estimate of the theoretical uncertainty of the cross section.

Thus, in addition to the usual output file `<outfile>`, running `SusHi_1.6.0` with the standard command

```
./bin/sushi <infile> <outfile>
```

will produce an additional file `<outfile>_murdep` which contains the gluon-fusion cross section for several values of μ_R in the form

$$\mu_\mathrm{R}/\mathrm{GeV} \qquad \sigma_\mathrm{LO}/\mathrm{pb} \qquad \sigma_\mathrm{NLO}/\mathrm{pb} \qquad \sigma_\mathrm{NNLO}/\mathrm{pb} \qquad \sigma_{\mathrm{N^3LO}}/\mathrm{pb} \tag{22}$$

where all cross sections are evaluated following Eq. (4), i.e. they potentially contain quark-mass effects, SUSY corrections, and/or electroweak effects. The values of μ_R to be scanned over can be set in `<infile>` through

```
Block SCALES
    1  <mu0mh>
  102  <min0>  <max0>  <N>
```

which will cause `SusHi_1.6.0` to evaluate the cross section at $N+1$ equidistant points for $\log\mu_\mathrm{R}$ between $\log\mu_\mathrm{min}$ and $\log\mu_\mathrm{max}$, meaning[8]

$$\mu_\mathrm{R} = \mu_\mathrm{min}\left(\frac{\mu_\mathrm{max}}{\mu_\mathrm{min}}\right)^{i/N}\,, \qquad i \in \{0,1,\ldots,N\}\,. \tag{23}$$

[8] `<N>`$=N$, `<min0>`$=\mu_\mathrm{min}/\mu_0$, `<max0>`$=\mu_\mathrm{max}/\mu_0$, `<mu0mh>`$=\mu_0/M_\phi$.

In addition, SusHi_1.6.0 includes a theoretical error estimate on the inclusive cross section into the standard output file <outfile>, given as the maximal and minimal deviation (in pb) within the interval $\mu_R \in [\mu_1, \mu_2]$ from the value at $\mu_R = \mu_0$. The interval is specified as SCALES(101)=$\{\mu_1/\mu_0, \mu_2/\mu_0\}$ (recall that μ_0/M_ϕ =SCALES(1)); it defaults to $[\mu_1, \mu_2] = [\mu_0/2, 2\mu_0]$.

We remark that this feature works at all perturbative orders through N^{3}LO, for any settings in the blocks GGHMT or GGHSOFT, and for any model under consideration. The only restriction is that all parameters except for the strong coupling constant need to be defined on-shell. If this is not the case, SusHi_1.6.0 will not produce <outfile>_murdep. Note that, due to Eq. (4), the procedure implemented in SusHi_1.6.0 is a slightly refined version of the one described above. In particular, this implies that the NNLO μ_R dependence is *exact*, since it is fully determined by the exact NLO cross section σ_{NLO}. On the other hand, the renormalization-scale dependence at N^{3}LO derived from the RGE procedure inherits whatever approximations were made (or not made) at NNLO. Thus, the result obtained through the standard and the RGE procedure are usually not identical. For example, if one keeps the full x-dependence at NNLO, one also obtains the full x-dependence of the μ_R-terms at N^{3}LO with the RGE procedure, while the standard procedure would only provide them in the soft expansion.

3.5. Effective Lagrangian - dimension-5 operators

Let us start from a particular well-defined theory TH; in the current version of SusHi, this could be the SM, a general 2HDM, the MSSM, or the NMSSM. We may now include additional gauge invariant dimension-5 operators to TH which couple the neutral Higgs bosons of TH to gluons in the following way[9]:

$$\mathcal{L} = \mathcal{L}_{\rm TH} + \sum_{i=1}^{N_1} \frac{\alpha_s}{12\pi v} c_{5,1i}\, H_{1i} G^a_{\mu\nu} G^{a,\mu\nu} + \sum_{i=1}^{N_2} \frac{\alpha_s}{8\pi v} c_{5,2i}\, H_{2i} G^a_{\mu\nu} \tilde{G}^{a,\mu\nu}\,. \tag{24}$$

Here, $\mathcal{L}_{\rm TH}$ is the Lagrangian of the initial theory TH, $G^a_{\mu\nu}$ is the gluonic field strength tensor with color index a and Lorentz indices μ and ν, and $\tilde{G}^a_{\mu\nu} \equiv \varepsilon_{\mu\nu\rho\sigma} G^{a,\rho\sigma}$ is its dual ($\varepsilon^{0123} = +1$). As usual, α_s is the strong coupling constant and v the SM Higgs-boson vacuum expectation value, which we express in terms of Fermi's constant $v = 1/\sqrt{\sqrt{2} G_F}$. N_1 and N_2 are the numbers of CP-even and CP-odd Higgs bosons of the theory, respectively. The particles themselves are generically denoted by H_{1i} and H_{2i} (cf. also Table 1 below).

The $c_{5,ni}$ denote dimensionless Wilson coefficients which are understood as perturbative series in α_s:

$$c_{5,ni} = \sum_{k=0}^{3} \left(\frac{\alpha_s}{\pi}\right)^k c^{(k)}_{5,ni}\,. \tag{25}$$

[9] CP-even and -odd scalars, which couple through dimension-5 operators only, can also be studied, see the description after Eq. (31).

<htype>	SM	2HDM/MSSM	NMSSM
11	H	h	H_1
12	–	H	H_2
13	–	–	H_3
21	A	A	A_1
22	–	–	A_2

Table 1: Assignment of the SusHi input parameter SUSHI(2)=<htype> to the type of Higgs boson in the various models. A dash (–) means that the assignment is not meaningful; it will lead to a fatal error in SusHi.

The normalization is such that $c^{(0)}_{5,ni} = 1$ corresponds to the LO contribution of an infinitely heavy up-type quark u' with SM-couplings.[10] The NLO term for a CP-even Higgs in this case would be $c^{(1)}_{5,11} = \frac{11}{4}$, etc. In a theory that obeys naturalness, on the other hand, the order of magnitude of the Wilson coefficients would be $c_{5,ni} = \mathcal{O}(v/\Lambda)$, where Λ is a scale of physics beyond the SM.

The basic structures for the implementation of the effective Lagrangian in Eq. (24) have already been present in earlier versions of SusHi. The reason for this is that the very same operators result from integrating out the top quark or heavy squarks and gluinos from $\mathcal{L}_{\rm TH}$. In fact, the NNLO corrections due to top quarks, as well as the NLO corrections due to top, stop, and gluino are evaluated on the basis of these dimension-5 operators.

Thus, SusHi_1.6.0 does not implement any new results; it simply re-uses previously available functions and subroutines in order to extend the gluon-fusion amplitudes to take into account the effect of the additional terms in Eq. (24). The numerical values for the coefficients $c_{5,ni}$ in Eq. (24) are specified through the newly introduced Block DIM5.

For example, within the MSSM,

```
Block DIM5
    11    1.00000000E-04    # c5h0
    12    4.00000000E-05    # c5H0
    21   -3.00000000E-07    # c5A0
```

corresponds to $c^{(0)}_{5,11} \equiv c^{(0)}_{5,h} = 10^{-4}$, $c^{(0)}_{5,12} \equiv c^{(0)}_{5,H} = 4 \cdot 10^{-5}$, and $c^{(0)}_{5,21} \equiv c^{(0)}_{5,A} = -3 \cdot 10^{-7}$. Note that SusHi calculates the cross section of only one particular type of Higgs boson per run (defined in SUSHI(2)), see Ref. [7]. Correspondingly, only the pertinent entry in Block DIM5 will have an effect on the result, the other entries will be ignored. The corrections at higher orders are specified by setting DIM5(<k><ni>) for coefficients $c^{(k)}_{5,ni}$ with $k \geq 1$. At NLO the contribution of an infinitely heavy up-type quark u' is thus reproduced by setting DIM5(11)=1 and DIM5(111)=2.75.

The scale dependence of the dimension-5 Wilson coefficient can be derived from the non-

[10] "SM-like" refers to the interaction Lagrangian $\mathcal{L}_{\rm int} = -(m_{u'}/v) H_{1i} \bar{u}' u'$ for a CP-even, and $\mathcal{L}_{\rm int} = -i(m_{u'}/v) H_{2i} \bar{u}' \gamma_5 u'$ for a CP-odd Higgs boson.

renormalization of the trace anomaly term [10, 95–98],

$$\mu^2 \frac{\mathrm{d}}{\mathrm{d}\mu^2} \beta(\alpha_s) G_{\mu\nu} G^{\mu\nu} \equiv 0\,, \tag{26}$$

where $\beta(\alpha_s)$ is given in Eq. (20). Since also $\alpha_s c_{5,1i} G_{\mu\nu} G^{\mu\nu}$ must be scale invariant, this immediately leads to

$$c_{5,1i}(\mu_\mathrm{R}) = c_{5,1i}(\mu_\phi) \frac{(\beta/\alpha_s)|_{\mu_\mathrm{R}}}{(\beta/\alpha_s)|_{\mu_\phi}}\,. \tag{27}$$

Perturbatively, we can write this as

$$c_{5,1i}(\mu_\mathrm{R}) = \sum_{n\geq 0} \sum_{l=0}^{n} \left(\frac{\alpha_s(\mu_\mathrm{R})}{\pi}\right)^n c_{5,1i}^{(n,l)}(\mu_\phi) l_{R\phi}^l\,, \tag{28}$$

with $l_{R\phi} = 2\ln(\mu_\mathrm{R}/\mu_\phi)$,

$$c_{5,1i}^{(n,0)} = c_{5,1i}^{(n)}(\mu_\phi)\,, \quad c_{5,1i}^{(n,n)} = 0 \qquad \forall\ n \tag{29}$$

and, through NNLO,

$$\begin{aligned} c_{5,1i}^{(2,1)} &= \beta_0 c_{5,1i}^{(1,0)} - \beta_1 c_{5,1i}^{(0,0)}\,, \\ c_{5,1i}^{(3,2)} &= \beta_0(\beta_0 c_{5,1i}^{(1,0)} - \beta_1 c_{5,1i}^{(0,0)})\,, \quad c_{5,1i}^{(3,1)} = 2(\beta_0 c_{5,1i}^{(2,0)} - \beta_2 c_{5,1i}^{(0,0)})\,. \end{aligned} \tag{30}$$

Setting `DIM5(0)=1` makes `SusHi` evolve the Wilson coefficient perturbatively, i.e. according to Eq. (28); this is the default. On the other hand, one can also employ Eq. (27) for the evolution by setting `DIM5(0)=2`, similar to the implementation in `Higlu` [10]. The evolution can also be switched off (i.e. $c_{5,1i}(\mu_\mathrm{R}) = c_{5,1i}(\mu_\phi)$) by setting `DIM5(0)=0`. The RGE procedure described in the previous section is only applicable for `DIM5(0)=1`. `SusHi` will assume the Wilson coefficient provided in the input `Block DIM5` to be renormalized at $\mu_\phi = M_\phi$. The corresponding values at μ_R (where μ_R is given in `SCALES(1)`) are output in `Block DIM5OUT`.

Moreover, the inclusion of dimension-5 operators is not compatible with the inclusion of $1/M_\mathrm{t}$ terms, i.e. `SusHi` stops if `GGHMT(1)`$\neq$`0` or `GGHMT(2)`$\neq$`0`. The LO dependence including quark-mass effects must not be factored out, i.e. `SusHi` only accepts the setting `GGHMT(-1)=-1`, in order not to reweight the dimension-5 operator contributions with top-quark mass effects.

We note that through the `Block FACTORS`, which existed also in earlier versions, `SusHi` allows to alter the couplings of the Higgs boson to quarks and squarks. Thus, for example additional factors κ_t and κ_b for the Higgs-boson coupling to top and bottom quarks can be chosen. In case of the SM the corresponding Lagrangian then takes the following form for the CP-even Higgs boson $H_{11} = H$

$$\mathcal{L}_\mathrm{TH} \ni -\kappa_t \sqrt{2} \frac{M_\mathrm{t}}{v} t\bar{t}H - \kappa_b \sqrt{2} \frac{M_\mathrm{b}}{v} b\bar{b}H\,. \tag{31}$$

It is therefore easily possible to perform an analysis as presented in Ref. [99] in SusHi, where the dependence of the gluon-fusion cross section on κ_t and $c_{5,1i}$ is discussed. We will later also focus on this dependence for a very boosted Higgs taking into account the bottom-quark induced contribution in addition. Moreover, by setting the couplings to quarks and gauge bosons to zero through the settings in Block FACTORS and SUSHI(7)=0, respectively, also CP-even or -odd scalars beyond the implemented models can be studied. We will demonstrate this option by providing inclusive cross sections for a scalar with a mass of 750 GeV at the 13 TeV LHC in Section 5.4.

4. Heavy-quark annihilation

In this section we shortly comment on the implementation of the total inclusive NNLO Higgs-production cross sections through heavy-quark annihilation, $Q'\bar{Q} \to \phi$, as described in Ref. [30]. Its activation is through the presence of the Block QQH in the input file, which has the following form:

```
Block QQH
         1      <parton1>
         2      <parton2>
        11      <v*y>
        12      <mu>
```

Here, <parton1>$\in \{1,\ldots,5\}$ denotes the initial-state quark flavor Q', and <parton2>$\in \{-1,\ldots,-5\}$ the initial-state anti-quark flavor $\bar{Q}$. <v*y> is the $Q'\bar{Q}\phi$ coupling in the $\overline{\text{MS}}$ scheme at scale <mu>$= \mu/\text{GeV}$, normalized such that the SM value of the $q\bar{q}H$ coupling is <v*y>$= m_q(\mu)/\text{GeV}$. For further details regarding the implementation in SusHi_1.6.0 and results we refer to Ref. [30].

If the Block QQH is provided, SusHi will not calculate the gluon-fusion cross section. The calculation of heavy-quark annihilation cross sections is also compatible with cuts on the (pseudo)rapidity or transverse momentum of the Higgs boson up to $\mathcal{O}(\alpha_s^3)$, controlled through the settings in Block DISTRIB. Also p_T distributions (DISTRIB(1)=1) can be requested. Since all quarks are assumed massless in this approach, the underlying theory is chirally symmetric. Therefore the results for a scalar and a pseudo-scalar Higgs are identical and the setting of SUSHI(2) is irrelevant. Note also that the collision of an up-type quark with a down-type anti-quark (or vice versa) implies that ϕ carries an electric charge. The only model dependence of the $Q'\bar{Q}\phi$ cross section as calculated by SusHi is through the setting of the Yukawa coupling in QQH(11), such that a calculation in the SM-mode is sufficient (SUSHI(1)=0), unless the Higgs mass should be obtained from some external code like FeynHiggs.

Other parameters of the $Q'\bar{Q}\phi$ calculation are determined by the same input values as they are used for the $b\bar{b}\phi$ cross section when no input Block QQH is present. In particular, the perturbative order of $Q'\bar{Q}\phi$ is controlled through SUSHI(6)=n, where $n = 1, 2, 3$ results in the LO, NLO, or NNLO prediction, respectively, and the renormalization and factorization scales (relative to M_ϕ) are defined through SCALES(11) and SCALES(12), respectively.

5. Numerical results

This section demonstrates the newly implemented features of `SusHi_1.6.0` with the help of exemplary numerical results. We start with a discussion of the convergence of the soft expansion at individual perturbative orders up to N^{3}LO, proceed with top-quark mass effects in the effective field-theory approach, move to the RGE procedure to determine the renormalization-scale dependence, before we use these features to provide a prediction for the cross section of the SM Higgs boson. Finally, we study the effect of higher dimensional operators to the transverse momentum p_T of the SM Higgs boson and provide inclusive cross sections for a CP-even scalar with a mass of 750 GeV. For numerical results concerning heavy-quark annihilation, we refer the reader to Ref. [30].

If not stated otherwise, the setup for the numerical evaluations is as follows: The LHC center-of-mass energy is set to $\sqrt{s} = 13\,\text{TeV}$, and the SM Higgs mass to $M_\text{H} = 125\,\text{GeV}$. We employ `PDF4LHC15` [100–106] as parton distribution functions (PDF), where the `(n)nlo_mc` Monte Carlo is used by default, and the `(n)nlo_100` Hessian sets if noted. Since N^{3}LO PDF sets are not available, we use the NNLO set also for the evaluation of the N^{3}LO terms. Nevertheless, in the N^{3}LO calculation, we evolve α_s at 4-loop level; using 3-loop running of α_s instead, the final prediction of the cross section for a SM Higgs boson changes at the level of 10^{-5}. The remaining input follows the recommendation of the LHC Higgs cross section working group, see Ref. [107]. The on-shell charm-quark mass is set to $m_c^\text{OS} = 1.64\,\text{GeV}$, which is the upper edge of the range given in Ref. [107]. The central scale choice for the renormalization and factorization scale is $\mu_\text{R} = \mu_\text{F} = M_\text{H}/2$.

Note that the results of Sections 5.1–5.3 are obtained for a SM Higgs boson. However, `SusHi_1.6.0` allows to take into account the effects of N^{3}LO contributions in the heavy-top limit and $1/M_\text{t}$ terms to the NNLO contributions for any CP-even Higgs boson in the implemented models, as long as the mass of the Higgs boson under consideration is sufficiently light, i.e. below $2M_\text{t}$. Effects of dimension-5 operators (see Section 3.5 and 5.4), on the other hand, can be taken into account for any of the neutral Higgs bosons of the implemented models and CP-even and -odd scalars, which couple through dimension-5 operators only.

5.1. Soft expansion up to N^{3}LO

In this section, we study the behavior of the expansion around the "soft limit", $x \to 1$, for the gluon-fusion cross section, see also Section 3.1. For the sake of clarity, top-quark mass effects beyond LO will be neglected in this section, although the LO cross section including the full top-quark mass dependence is factored out to all orders (i.e. we set `GGHMT(-1)=3`, see Section 3.3). In order to discuss the convergence of the soft expansion, we define the quantity

$$\left(\frac{\delta\sigma}{\sigma}\right)^{\text{N}^n\text{LO}} = \frac{\sigma^t_{\text{N}^n\text{LO},N,a}}{\sigma^t_{\text{N}^{n-1}\text{LO}}} - 1 \quad \text{with } n \geq 1\,, \tag{32}$$

where $\sigma^t_{\text{N}^n\text{LO}}$ has been introduced in Eq. (5). Through $\mathcal{O}(\alpha_s^{n+1})$, the exact x-dependence is taken into account. In the highest-order terms, i.e. the terms of order $\mathcal{O}(\alpha_s^{n+2})$ in $\sigma^t_{\text{N}^n\text{LO},N,a}$,

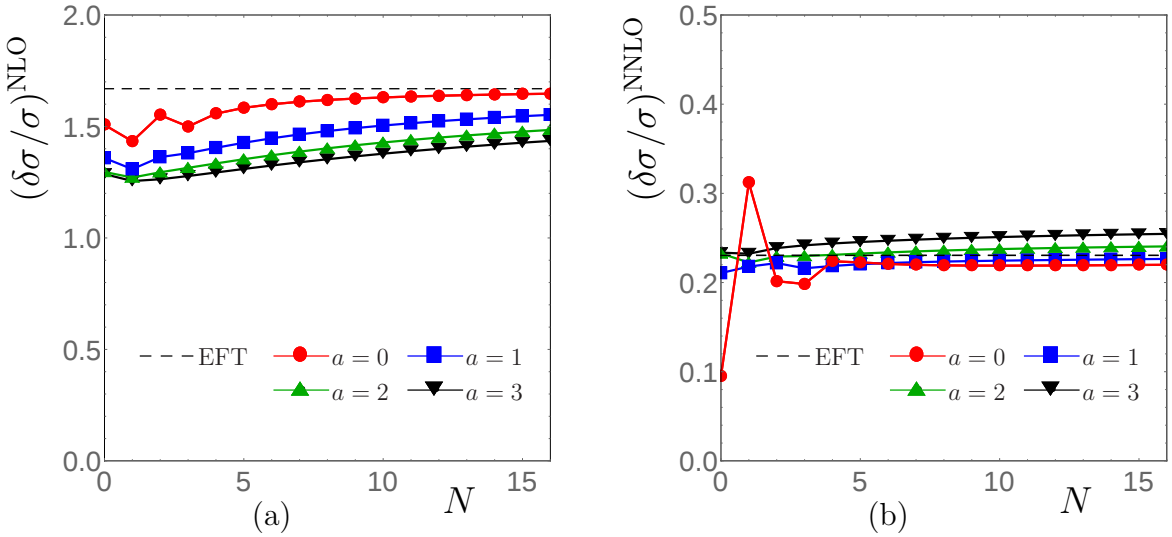

Figure 2: (a) Convergence of the NLO cross section as a function of N for $a = 0, 1, 2, 3$ in Eq. (5); (b) Convergence of the NNLO cross section as a function of N for $a = 0, 1, 2, 3$ in Eq. (5). In both figures the colors depict $a = 0$ (red), $a = 1$ (blue), $a = 2$ (green), $a = 3$ (black). The black, dashed line corresponds to the exact result in the heavy-top limit. The results are obtained for a SM Higgs with $M_{\mathrm{H}} = 125\,\mathrm{GeV}$ at the $\sqrt{s} = 13\,\mathrm{TeV}$ LHC.

the soft expansion is applied according to Eq. (5) up to order $(1-x)^N$ with $N \leq 16$. All studies in this subsection were performed without matching the cross section to the result at $x \to 0$, i.e., we set `GGHMT(`n`·10)=0` for $n = 1, 2, 3$.

At infinite order of the soft expansion, the value of the parameter a in Eq. (5) is obviously irrelevant. If only a finite number of terms in the expansion is available, the dependence of the result on the parameter a has been studied in detail in Ref. [22]. It was shown that the soft expansion seems to converge particularly well for small, non-negative values of a. The differences among the final results for different values of a are smaller at higher orders, as we demonstrate subsequently. One observes that the μ_{F}-dependent terms of $\hat{\sigma}$ at NLO are polynomial in x, which means that they are *identical* to their soft expansion for $a = 0$ once it is taken to sufficiently high order ($N = 3$, to be specific). This is no longer true with the choice $a > 0$. Let us add that, since the μ_{R}-dependent terms at NLO are proportional to $\delta(1-x)$, they are the same whether the soft expansion is applied or not.

Figs. 2 (a) and (b) show the convergence of the soft expansion at NLO and NNLO, respectively. Both figures also include the result without soft expansion as dashed black line, i.e. where $\sigma^{t}_{\mathrm{N^nLO},N,a}$ is replaced by $\sigma^{t}_{\mathrm{N^nLO}}$ in Eq. (32). At NLO, the case $a = 0$ appears to be clearly preferable; for larger value of a, the soft expansion is further away from the exact x-dependence. For $N \geq 9$, the deviation for $a = 0$ is less than 2.5%.[11] It decreases down to 1.3% at $N = 16$, while the result for $a = 1$ is still more than 7% off.

At NNLO, convergence of the soft expansion appears to be a bit faster, with no significant

[11] Note that this refers to the absolute NLO *correction* term in pb; with respect to the total cross section, this translates into an approximation which is better than 1.6%.

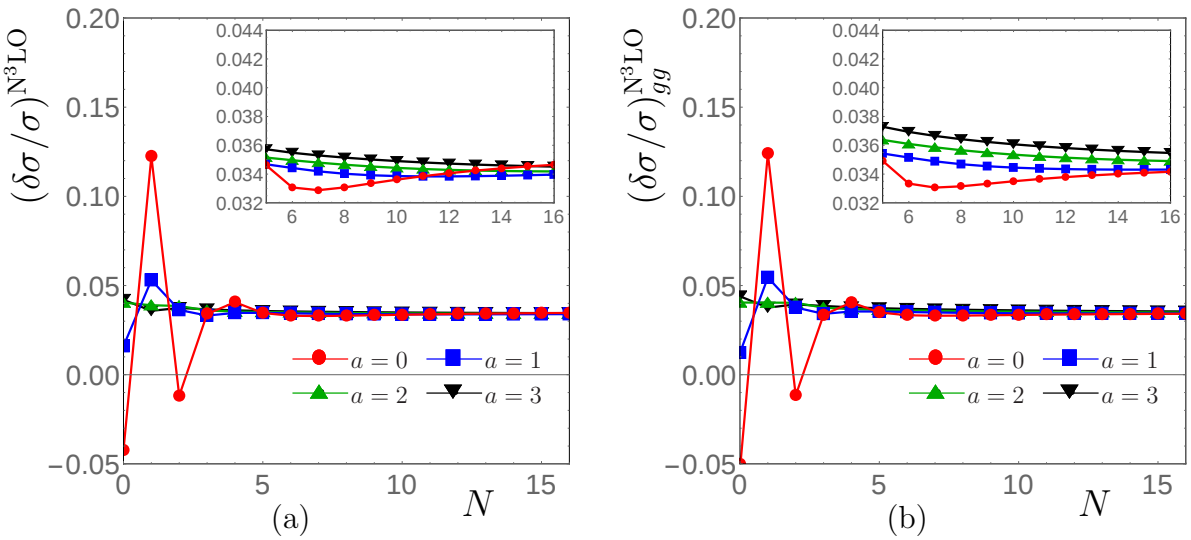

Figure 3: (a) Convergence of the N^{3}LO cross section as a function of N for $a = 0, 1, 2, 3$ in Eq. (5); (b) Convergence of the gg channel of the N^{3}LO as a function of N for $a = 0, 1, 2, 3$ in Eq. (5). A zoom for larger values of N is provided in the upper right corner of the figures. In both figures the colors depict $a = 0$ (red), $a = 1$ (blue), $a = 2$ (green), $a = 3$ (black). The results are obtained for a SM Higgs with $M_{\mathrm{H}} = 125\,\mathrm{GeV}$ at the $\sqrt{s} = 13\,\mathrm{TeV}$ LHC.

impact of the terms higher than $(1-x)^6$ both for $a = 0$ and $a = 1$. For $N \geq 9$, the result for $a = 0$ ($a = 1$) approximates the exact x-dependence of the correction term to better than 5% (2%) (translating into about 0.9% (0.3%) for the total cross section).

Fig. 3 (a) depicts the convergence of the soft expansion for the cross section at N^{3}LO. Above $N = 11$, the spread among the curves for $a = 0, 1, 2, 3$ is of the order of 3% of $\delta\sigma/\sigma$, which means about 0.1% of the total cross section. For completeness, the same plot for the dominant gg channel alone is shown in Fig. 3 (b). Note that in this case, we only include the gg channel also in the denominator of Eq. (32). At lower orders of the soft expansion, the curve for $a = 0$ behaves less smoothly compared to $a \geq 1$; at sufficiently high orders though, all results can be considered consistent with each other at the level of accuracy indicated above.

5.2. Top-quark mass effects through NNLO and matching to the high-energy limit

In this section we comment on top-quark mass effects beyond the heavy-top limit, which can be taken into account in `SusHi` up to $1/M_{\mathrm{t}}^{10}$ at LO and NLO and up to $1/M_{\mathrm{t}}^{6}$ at NNLO. As already pointed out in Section 3.3, a naive expansion of the partonic cross section in $1/M_{\mathrm{t}}$ breaks down. Thus, in this section, we apply the matching to the high-energy limit as described in Section 3.3, i.e. we set `GGHMT(`n`·10)=1` for $n = 1, 2, 3$.

Recall that the matching procedure of Refs. [24, 25] requires the soft expansion of the partonic cross section. Thus before discussing the relevance of the top-quark mass effects, it is necessary to study the convergence of the soft expansion also for these terms. For the result at NLO we can compare to the result in the heavy-top limit, but also to the exact top-quark

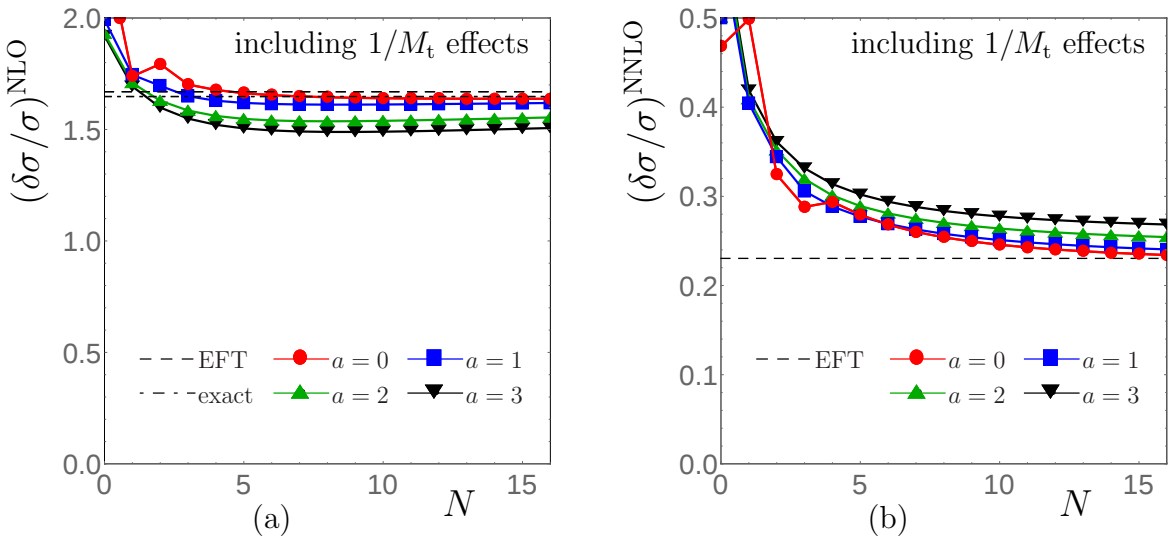

Figure 4: (a) Convergence of the NLO cross section as a function of N for $a = 0, 1, 2, 3$ in Eq. (5) with top-quark mass effects up to $1/M_t^8$; (b) Convergence of the NNLO cross section as a function of N for $a = 0, 1, 2, 3$ in Eq. (5) with top-quark mass effects up to $1/M_t^4$. In both figures the colors depict $a = 0$ (red), $a = 1$ (blue), $a = 2$ (green), $a = 3$ (black). The black, dashed line corresponds to the exact result in the heavy-top limit, the black, dot-dashed line to the exact result with full top-quark mass dependence (only known at NLO). The results are obtained for a SM Higgs with $M_H = 125\,\text{GeV}$ at the $\sqrt{s} = 13\,\text{TeV}$ LHC.

mass dependence; the difference between these two results is about 1%. At NNLO, on the other hand, only a comparison to the heavy-top limit is possible. The results are shown in Fig. 4, including terms through $1/M_t^8$ at NLO, and through $1/M_t^4$ at NNLO (for the gg and the qg channels also $1/M_t^6$ terms are implemented in `SusHi` but provide a negligible contribution, see Fig. 6 below). Following Eq. (32), we keep the exact x-dependence one order below to allow for a better comparison with the figures of Section 5.1. At NLO, one observes a nice convergence of the soft expansion to the exact result, provided $a = 0$. Terms beyond $(1 - x)^{10}$ have only negligible effects on the final result in this case. At NNLO, convergence of the soft expansion is significantly slower, but the available number of terms in this expansion seems sufficient for a prediction of the mass effects with permille level accuracy, provided that $a = 0$ is indeed the most reliable choice for the parameter defined in Eq. (5). Fig. 5 shows the N^{3}LO result with matching to the high-energy limit as described in Section 3.3. The convergence of the soft expansion as a function of N is slightly worse compared to the result without matching, but shows a similar behaviour as the results at NLO and NNLO depicted in Fig. 4. The correction at $N = 16$ is comparable to the result without matching, see Fig. 3.

Let us now discuss the top-quark mass effects at different orders $1/M_t^P$ in more detail, while applying the soft expansion through $(1-x)^{16}$ with $a = 0$ (see Eq. (5)). The result is presented in Fig. 6, where the relative difference

$$\left(\frac{\delta\sigma}{\sigma}\right)_{M_t} = \frac{\sigma_P}{\sigma_{\rm htl}} - 1 \tag{33}$$

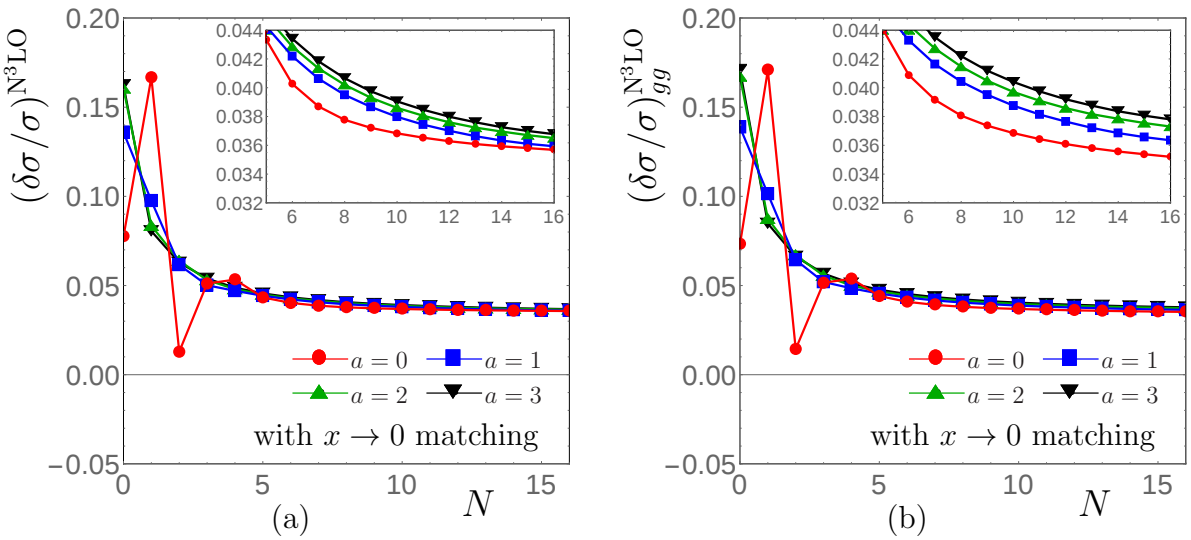

Figure 5: (a) Convergence of the N^{3}LO cross section as a function of N for $a = 0, 1, 2, 3$ in Eq. (5); (b) Convergence of the gg channel of the N^{3}LO as a function of N for $a = 0, 1, 2, 3$ in Eq. (5). A zoom for larger values of N is provided in the upper right corner of the figures. In both figures the colors depict $a = 0$ (red), $a = 1$ (blue), $a = 2$ (green), $a = 3$ (black). In contrast to Fig. 3 the N^{3}LO result is matched to the high-energy limit. The results are obtained for a SM Higgs with $M_{\mathrm{H}} = 125\,\mathrm{GeV}$ at the $\sqrt{s} = 13\,\mathrm{TeV}$ LHC.

to the heavy-top limit at the corresponding perturbative order is shown. At NLO, σ_P is obtained by including terms of order $1/M_{\mathrm{t}}^P$ in the partonic cross section and matching it to the $x \to 0$ limit (i.e. `GGHMT(1)=`P, `GGHMT(10)=1`, `GGHSOFT(1)={1,16,0}`), while σ_{htl} is the heavy-top limit at NLO (i.e. `GGHMT(1)=GGHMT(10)=0`, `GGHSOFT(1)={0,0,0}`). In both cases, the value for the cross section provided by `SusHi` in `XSGGHEFF(1)` is used.

At NNLO, we use Eq. (4) which corresponds to the `SusHi` output `SUSHIggh(1)`, neglecting bottom- and charm-quark, and electroweak effects (`FACTORS(1)=FACTORS(3)=SUSHI(7)=0`). Furthermore, we make sure that only the genuine NNLO effects of the $1/M_{\mathrm{t}}$ terms are shown, by fixing the approximation used at $\mathcal{O}(\alpha_s^3)$; specifically, we set `GGHMT(1)=6`, `GGHMT(10)=1`, and `GGHSOFT(1)={1,16,0}`, both for σ_P and σ_{htl}. For the $\mathcal{O}(\alpha_s^4)$-terms, we apply the analogous settings of the NLO case described above. I.e., we include terms of order $1/M_{\mathrm{t}}^P$ in σ_P (modulo the restriction to $1/M_{\mathrm{t}}^4$ for the pure quark channels, see above), and match them to the $x \to 0$ limit, while we apply the usual heavy-top limit for σ_{htl}.

The results are shown in Fig. 6, together with the relative difference of the *exact* NLO cross section to its heavy-top limit (black dashed). The points at $P = 0$ illustrate the effect of using the soft expansion combined with matching to the result at $x = 0$, as opposed to keeping the full x dependence (without matching). Both at NLO and NNLO, this effect is obviously larger than the genuine $1/M_{\mathrm{t}}$-terms. This underlines that, as long as one works in a heavy-top approximation, which is strictly valid only for $x > M_\phi^2/(4M_{\mathrm{t}}^2)$, the full x-dependence is not necessarily an improvement w.r.t. the soft expansion, in particular if additional information like the $x \to 0$ limit is available.

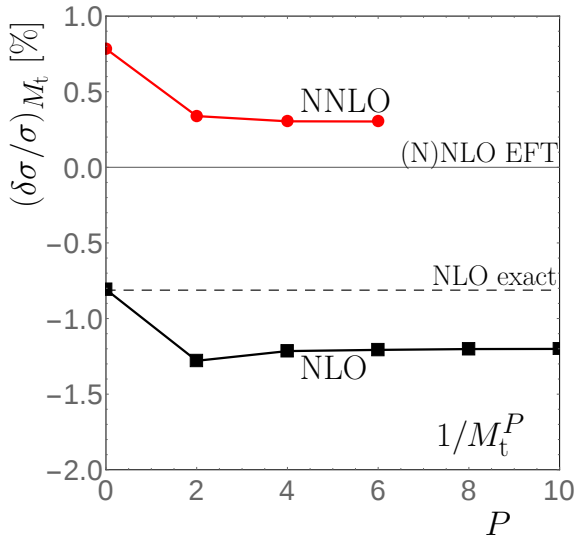

Figure 6: Relevance of $1/M_t^P$ terms to the cross section in the heavy-top limit in percent at NLO (black) up to $P = 10$ and at NNLO (red) up to $P = 6$ with respect to the exact heavy-top limit at the corresponding order. The black, dashed line corresponds to the exact NLO result. The results are obtained for a SM Higgs with $M_H = 125\,\text{GeV}$ at the $\sqrt{s} = 13\,\text{TeV}$ LHC.

Both at NLO and NNLO, the $1/M_t$ terms exhibit a nice convergence behavior. However, the observation at NLO is that, while the $1/M_t^0$ result almost exactly reproduces the full mass dependence, including higher-order mass effects moves the approximation *away* from the exact result. Thus, we cannot expect that their inclusion at NNLO leads to an improved result w.r.t. the heavy-top limit. Nevertheless, we believe that their overall behavior allows to derive an upper bound on the top-mass effects to the heavy-top limit of the order of 1% [24, 25, 27].

5.3. Cross section prediction for the SM Higgs boson and scale dependence

Having discussed the top-quark mass terms to the NLO and NNLO cross section in the heavy-top limit and the convergence of the soft expansion, we can finally provide a prediction for the cross section of the SM Higgs boson including its scale uncertainty. In this section we make use of the Hessian PDF sets `PDF4LHC15_(n)nlo_100`. Following the arguments of the preceding sections, the best prediction of `SusHi` is obtained with the following settings: use the perturbative result through N^{3}LO, i.e. set `SUSHI(5)=3`; at each order of the effective-theory result, apply the soft expansion through $(1-x)^{16}$ with $a = 0$, i.e. set `GGHSOFT(`n`)={1,16,0}` for $n \in \{1, 2, 3\}$; take into account top-quark mass terms to the predictions of the NLO and NNLO cross sections in the heavy-top limit through the settings `GGHMT(`n`)=4` for $n \in \{1, 2\}$, i.e. $1/M_t^4$ terms are taken into account at NLO and NNLO; match to the high-energy limit $x \to 0$ at NLO, NNLO, and N^{3}LO, i.e. set `GGHMT(`n`·10)=1` for $n = 1, 2, 3$. The choice of $a = 0$ is motivated through the reproduction of the correct scale dependence at NLO and the observations in Section 5. Also note that for all predictions in

the effective field-theory approach, we factor out the full top-quark mass dependence, i.e. `GGHMT(-1)=3`. Finally, we include the electroweak correction factor according to Eq. (4), i.e. we set `SUSHI(7)=2`. The exact NLO cross section of Eq. (4) contains the contributions from the three heaviest quarks: top, bottom, and charm. The numbers can be reproduced with the input file `SM-N3LO_best.in` in the `/example` folder of the `SusHi_1.6.0` distribution.

With this setup, we obtain

$$\begin{aligned}
\text{NNLO}: &\quad \sigma = 43.55\,\text{pb} \pm 4.44\,\text{pb}(\mu_\text{R})\,,\\
+\text{N}^3\text{LO}: &\quad \sigma = 45.20\,\text{pb} \pm 1.61\,\text{pb}(\mu_\text{R})\,,\\
+1/M_\text{t}\ \text{effects at NLO and NNLO} & \qquad (34)\\
+\text{matching}\ (x \to 0)\ \text{at NLO, NNLO and N}^3\text{LO}: &\quad \sigma = 45.80\,\text{pb} \pm 1.87\,\text{pb}(\mu_\text{R})\,,\\
+\text{electroweak corrections}: &\quad \sigma = 48.28\,\text{pb} \pm 1.97\,\text{pb}(\mu_\text{R})\,,
\end{aligned}$$

where the uncertainty $\pm\Delta(\mu_\text{R})$ only takes into account the renormalization-scale dependence. Here, $\Delta(\mu_\text{R})$ is the maximum deviation of the cross section within the interval $\mu_\text{R}/M_\text{H} \in [1/4, 1]$ from the value at $\mu_\text{R} = M_\text{H}/2$. Each line of Eq. (34), including the uncertainty, has been obtained in a single run of `SusHi`, which takes a few seconds on a modern desktop computer. The final result is perfectly consistent within its uncertainties with the prediction $48.58\,\text{pb} \pm 1\,\text{pb}(\mu_\text{R})$ given in Ref. [22] and the result $48.1\,\text{pb} \pm 2.0\,\text{pb}$ (without resummation) employing the Cacciari-Houdeau Bayesian approach [108] to estimate higher unknown orders presented in Ref. [18]. We note that the result of Ref. [22] was computed with the NNLO PDF set at all orders, whereas we employ the NLO PDF set for the NLO terms in Eq. (4). If we employ `PDF4LHC15_nnlo_100` instead at all orders, we obtain 48.37 pb. Other uncertainties need to be added as described in Refs. [6, 22].

Running the input file `SM-N3LO_best.in` also generates a file including the renormalization-scale dependence. Its content is shown in Fig. 7 (a). The dependence clearly reduces successively at each order from LO to N^{3}LO. Note that at each order we follow Eq. (4) and thus include the electroweak correction factor beyond LO. The flat behavior around $\mu_\text{R} = M_\text{H}/2$ leads to a highly asymmetric scale variation around the central value, suggesting a symmetrization of the corresponding uncertainty band as done in Eq. (34). As explained in Section 3.4, the μ_R dependence obtained through the RGE procedure at N^{n}LO is as precise as the calculation at N^{n-1}LO, while in the standard procedure (by manually varying `SCALES(1)`), its precision is determined by the N^{n}LO calculation. We show the result of the standard procedure in Fig. 7 (b) (black lines). In addition, the $\mu = \mu_\text{F}$ dependence for $\mu_\text{R} = M_\text{H}/2$ (blue) and the combined $\mu = \mu_\text{F} = \mu_\text{R}$ dependence (red) are shown. In each case, the solid and dashed line corresponds to setting $a = 0$ and $a = 1$ in Eq. (5), respectively. The differences between these two cases, as well as between the standard and the RGE procedure are small, except for small values of μ. We also observe that the behaviour at low values of μ in Fig. 7 (b) is dependent on the soft expansion and the matching performed at NLO and NNLO. However, within the interval $\mu \in [M_\text{H}/4, M_\text{H}]$ which we use for the uncertainty determination, the agreement is good.

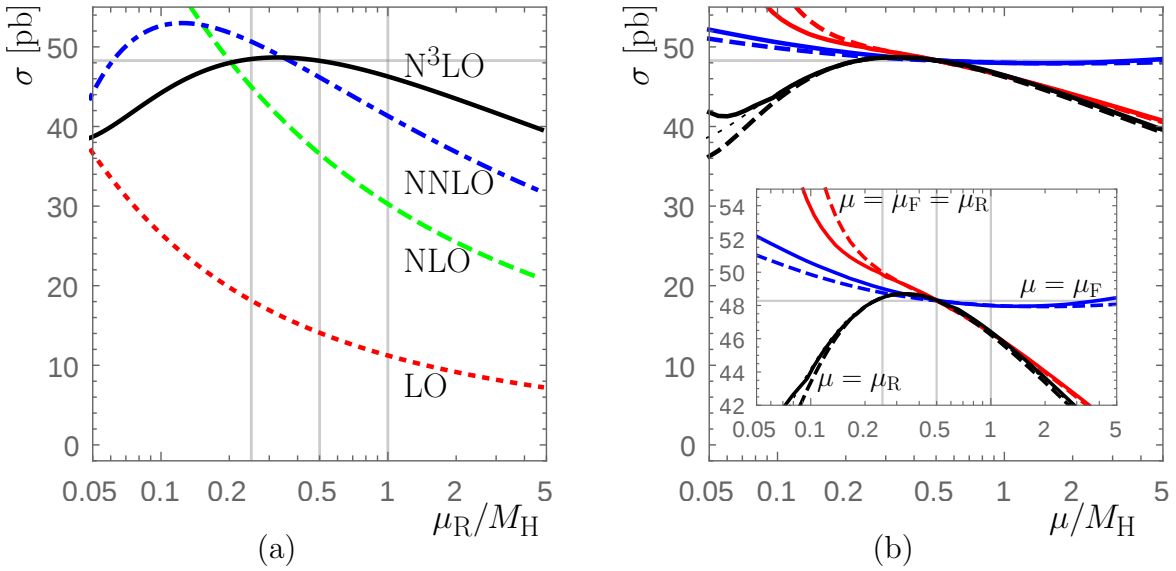

Figure 7: (a) LO (red, dotted), NLO (green, dashed), NNLO (blue, dotdashed) and N^{3}LO (black, solid) gluon-fusion cross section in pb (see Eq. (4)) as a function of μ_R/M_H (obtained in a single run); (b) Best prediction cross section in pb as a function of μ_F/M_H (together with $\mu_R = M_H/2$) (blue) and $\mu_F/M_H = \mu_R/M_H$ (red) and μ_R/M_H (together with $\mu_F = M_H/2$) (black). Each curve is shown twice, once for $a = 0$ (solid) and $a = 1$ (dashed) in the soft expansion at N^{3}LO. The dotted, thin black line depicts the N^{3}LO result from (a). Both figures are obtained for a SM Higgs with $M_H = 125\,\text{GeV}$ at the $\sqrt{s} = 13\,\text{TeV}$ LHC.

5.4. Dimension 5 operators

In order to study the effect of the dimension-5 operators, it is helpful to consider the fraction of events where the SM Higgs boson is produced at transverse momenta above a certain value p_T^{cut}. We define

$$R(p_T^{\text{cut}}) = \frac{1}{\sigma^{\text{tot}}}\sigma(p_T^{\text{cut}}) \quad \text{with} \quad \sigma(p_T^{\text{cut}}) = \int_{p_T > p_T^{\text{cut}}} \mathrm{d}p_T \frac{\mathrm{d}\sigma}{\mathrm{d}p_T}\,, \tag{35}$$

where $\sigma \equiv \sigma_{ni}(c_{5,ni})$ denotes the cross section for the production of a Higgs boson H_{ni} within the theory defined by Eq. (24), and follow the numerical setup described at the beginning of Section 5. However, we do not take into account charm-quark and electroweak contributions and choose a p_T-dependent renormalization and factorization scale for the result presented in Fig. 10. If not stated otherwise, the relative Yukawa couplings to top- and bottom quarks are set to one, i.e. we discuss the specific model TH with additional dimension-5 operator. In the subsequent NLO analysis, we set $c_5^{(1)} = \frac{11}{4}c_5^{(0)}$, i.e. our dimension-5 operator assumes the same (rescaled) NLO correction as for the top-quark induced Wilson coefficient.

The ratio $R(p_T^{\text{cut}})$ of Eq. (35) is shown in Fig. 8 for the SM Higgs boson as a function of (a) p_T^{cut} for various values of $c_{5,H}^{(0)}$, and (b) $c_{5,H}^{(0)}$ for various values of p_T^{cut}. Similarly, Fig. 9 shows the ratio for a CP-odd Higgs boson with mass 125 GeV. For Fig. 8 (a) and Fig. 9 (a), σ^{tot} is chosen such that each $R(p_T^{\text{cut}})$ is normalized to its NLO inclusive cross section. For Fig. 8 (b) and Fig. 9 (b), $\sigma^{\text{tot}} = \sigma(p_T^{\text{cut}})$ for $c_5 = 0$ to ensure that all curves start at one.

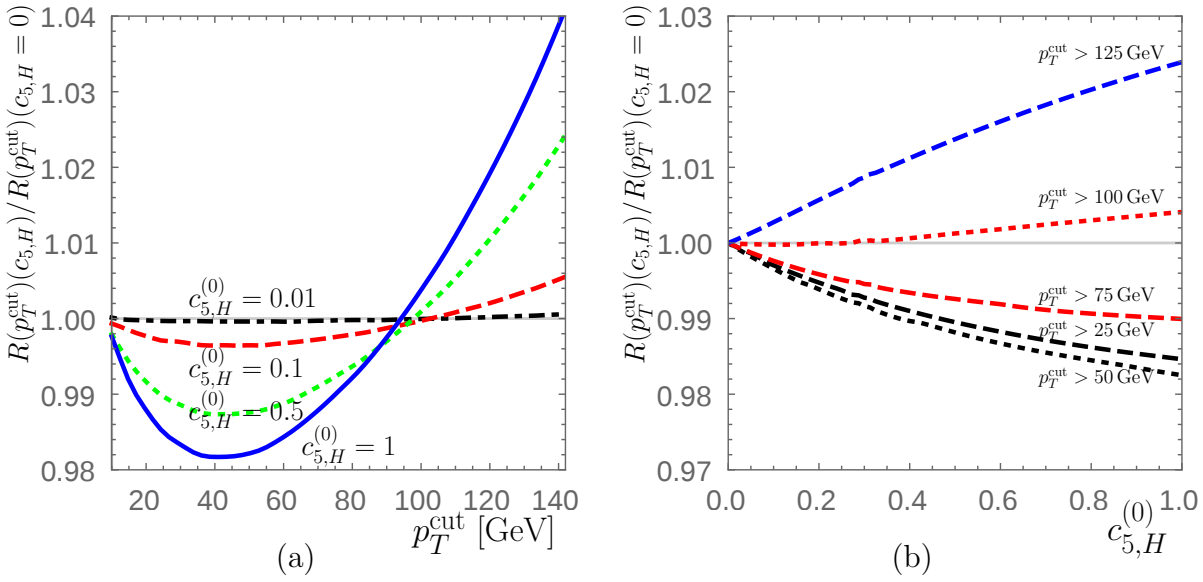

Figure 8: (a) Ratio of $R(p_T^{\rm cut})$ with different $c_{5,H}^{(0)}$ (see figure) and $R(p_T^{\rm cut})$ with $c_{5,H}=0$ as a function of $p_T^{\rm cut}$ in GeV; (b) Ratio of $R(p_T^{\rm cut})$ and $R(p_T^{\rm cut})$ with $c_{5,H}=0$ as a function of $c_{5,H}^{(0)}$ for different $p_T^{\rm cut}$ (see figure). In both figures we set $c_{5,A}^{(1)}=\frac{11}{4}c_{5,A}^{(0)}$. Both figures are obtained for a CP-even SM Higgs with $M_{\rm H}=125\,{\rm GeV}$ at the $\sqrt{s}=13\,{\rm TeV}$ LHC.

The minima, which are clearly visible around $p_T^{\rm cut}=50\,{\rm GeV}$, are induced by the negative interference with the bottom-quark induced contributions to gluon fusion, which turns into a positive interference for higher values of $p_T^{\rm cut}$. Accordingly, these minima affect also the dependence on c_5 in Fig. 8 (b) and Fig. 9 (b), i.e. the lowest curve is obtained for a value of $p_T^{\rm cut}$ around 40 GeV. Apart from the impact on the inclusive cross section, the point-like interaction encoded in the coefficient c_5 thus distorts the shape of the p_T distributions with respect to the loop-induced massive top- and bottom-quark contributions, as expected.

Following the study performed in Ref. [99], we now work out the dependence of the cross section with a minimal cut on p_T on the factors κ_t and $c_{5,H}^{(0)}$ for the SM Higgs boson[12]. In addition, we include the dependence on the bottom-quark induced contribution through the factor κ_b, since the latter is non-negligible for $p_T^{\rm cut}<200\,{\rm GeV}$. For this study we also choose p_T-dependent renormalization and factorization scales $\mu_{\rm R}=\mu_{\rm F}=\sqrt{M_{\rm H}^2+p_T^2}/2$, which is possible through the setting `SCALES(3)=1`. We define $\tilde{\sigma}(p_T^{\rm cut})$, which just includes the top-quark induced contribution, i.e. we set $\kappa_t=1$ and $c_{5,H}=\kappa_b=0$, and then perform a fit of

$$\frac{\sigma(p_T^{\rm cut})}{\tilde{\sigma}(p_T^{\rm cut})}=(\kappa_t+c_{5,H}^{(0)})^2+\delta\kappa_t c_{5,H}^{(0)}+\epsilon(c_{5,H}^{(0)})^2+\delta_{bt}\kappa_b\kappa_t+\delta_{bg}\kappa_b c_{5,H}^{(0)}+\epsilon_b\kappa_b^2\,, \tag{36}$$

where we set $c_{5,H}^{(1)}=\frac{11}{4}c_{5,H}^{(0)}$ and δ and ϵ are defined identically to Ref. [99]. In addition, however, we include the bottom-quark induced contribution, which is understood as pure

[12] Our $c_{5,H}^{(0)}$ corresponds to κ_g in Ref. [99].

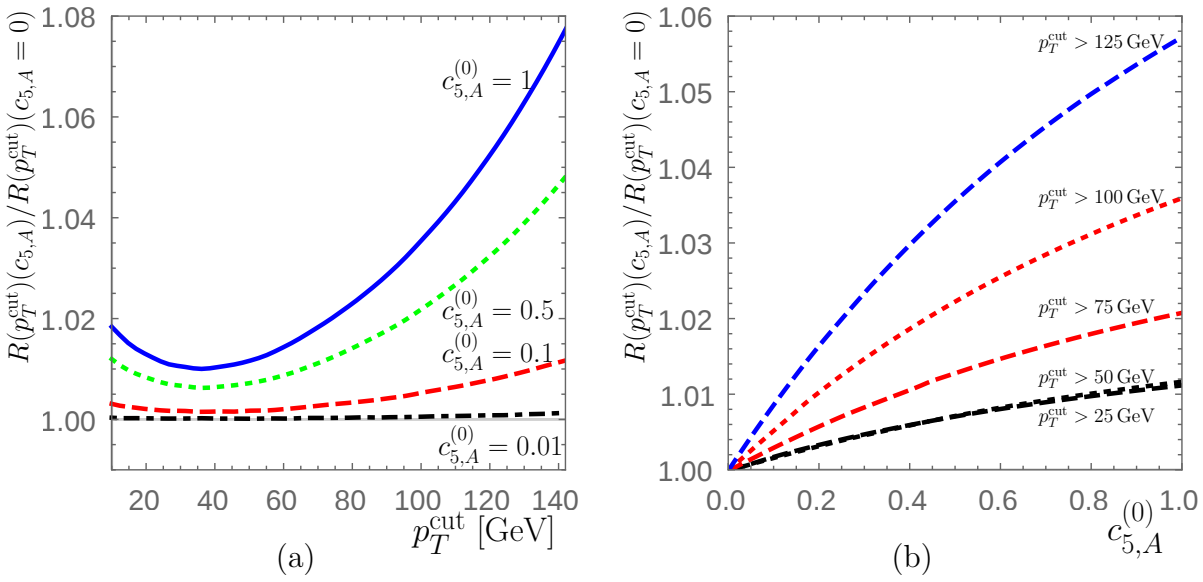

Figure 9: (a) Ratio of $R(p_T^{\rm cut})$ with different $c_{5,A}^{(0)}$ (see figure) and $R(p_T^{\rm cut})$ with $c_{5,A}=0$ as a function of $p_T^{\rm cut}$ in GeV; (b) Ratio of $R(p_T^{\rm cut})$ and $R(p_T^{\rm cut})$ with $c_{5,A}=0$ as a function of $c_{5,A}^{(0)}$ for different $p_T^{\rm cut}$ (see figure). In both figures we set $c_{5,A}^{(1)}=\frac{11}{4}c_{5,A}^{(0)}$. Both figures are obtained for a CP-odd Higgs with $m_A=125\,\text{GeV}$ at the $\sqrt{s}=13\,\text{TeV}$ LHC.

correction entering through δ_{bg}, δ_{bt}, and ϵ_b. The values for δ and ϵ coincide at the percent level with the values of Table 1 in Ref. [99], where for completeness we note that our calculation also includes the qq induced contribution to gluon fusion. For our numerical setup we show the dependence of the five correction factors on the lower cut $p_T^{\rm cut}$ in Fig. 10.

As it can be seen in Fig. 10 (a), the larger the lower cut $p_T^{\rm cut}$, the more the degeneracy between κ_t and $c_{5,H}$, which are indistinguishable in the inclusive cross section, is broken. On the other hand Fig. 10 (b) points out that for low $p_T^{\rm cut} < 200\,\text{GeV}$ bottom-quark induced contributions should also be taken into account. The interferences of the latter with the top-quark induced contributions on the one hand and with the effective coupling $c_{5,H}$ on the other hand, encoded in δ_{bt} and δ_{bg}, are identical only for low $p_T^{\rm cut}$. We note that the cross section prediction for the SM Higgs boson of course should include the full correction by bottom quarks given by δ_{bt} and ϵ_b. For completeness we partially also reproduced Fig. 2 of Ref. [99], which illustrates the disentanglement of the degeneracy between κ_t and $c_{5,H}$.

As a last example we discuss the calculation of the gluon-fusion cross section for an arbitrary scalar, which couples to gluons through an effective operator $c_5^{(0)}=1$ only. Motivated by the background deviation in the diphoton channel at 750 GeV in both LHC experiments [109, 110], we choose the mass of the scalar to be $m_X=750\,\text{GeV}$. We pick an input file for the SM, set the SM Higgs-boson mass to $M_{\rm H}=750\,\text{GeV}$, include a dimension-5 operator through `DIM5(11)=1`, but set the SM Higgs-boson couplings to quarks and gauge bosons to zero in `Block FACTORS` and through `SUSHI(7)=0`. The results are shown in Tab. 2. We include the renormalization scale uncertainty $\pm\Delta(\mu_{\rm R})$, which was obtained simultane-

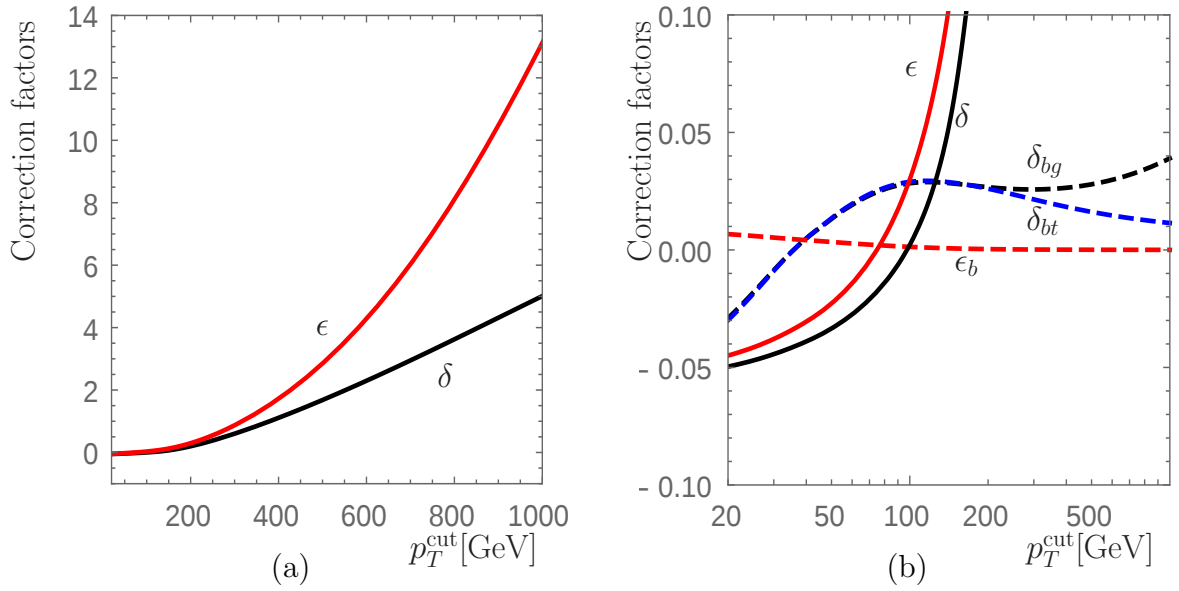

Figure 10: (a) Correction factors δ, ϵ as a function of the lower cut $p_T^{\rm cut}$ in GeV and in addition (b) δ_{bg}, δ_{bt} and ϵ_b as a function of $p_T^{\rm cut}$. Both figures are obtained for a SM Higgs with $M_{\rm H} = 125\,\text{GeV}$ at the $\sqrt{s} = 13\,\text{TeV}$ LHC.

ously. Again $\Delta(\mu_{\rm R})$ is the maximum deviation of the cross section within the interval $\mu_{\rm R} \in [1/4, 1]m_X$ and $\mu_{\rm R} \in [1/2, 2]m_X$ for the central scale choices $\mu_{\rm R} = \mu_{\rm F} = m_X/2$ and $\mu_{\rm R} = \mu_{\rm F} = m_X$, respectively. For this purpose the Wilson coefficient is evolved perturbatively, i.e. `DIM5(0)=1`. At N^{3}LO the soft expansion is performed up to $(1-x)^{16}$ with $a = 0$. The matching to the high-energy limit, $x \to 0$, is not applied. Similar to the SM Higgs boson we observe a good convergence of the perturbative series with a renormalization scale uncertainty of less than ± 1.3 and $\pm 2.9\%$ at N^{3}LO QCD for the central scale choices $\mu_{\rm R} = \mu_{\rm F} = m_X/2$ and $\mu_{\rm R} = \mu_{\rm F} = m_X$, respectively.

$\sigma(gg \to X)[fb]$	$\mu_{\rm R} = \mu_{\rm F} = m_X/2$	$\mu_{\rm R} = \mu_{\rm F} = m_X$
LO	246.2 ± 52.8	185.8 ± 36.0
NLO	368.7 ± 43.1	316.3 ± 39.1
NNLO	410.0 ± 19.1	384.9 ± 24.0
N^{3}LO	414.4 ± 5.3	407.2 ± 11.7

Table 2: Inclusive gluon-fusion cross section in fb for a CP-even scalar with mass $m_X = 750\,\text{GeV}$, which couples to gluons through $c_5^{(0)} = 1$ only. The results are given at different orders N^{k}LO, $k = 0, 1, 2, 3$, in QCD for the $\sqrt{s} = 13\,\text{TeV}$ LHC for two renormalization and factorization scale choices. The depicted uncertainty is the renormalization-scale uncertainty $\pm\Delta(\mu_{\rm R})$.

6. Conclusions

We presented the new features implemented in version `1.6.0` of the code `SusHi`. Aside from the implementation of heavy-quark annihilation, many new features aim at the improvement of the gluon-fusion cross-section prediction and its associated uncertainty estimate. In particular, `SusHi` now provides the soft expansion around the threshold of Higgs production and the matching to the high-energy limit for CP-even Higgs bosons, at NLO, NNLO and N^{3}LO QCD. Top-quark mass effects beyond the usual infinite top-mass limit can be taken into account at NLO and NNLO. We investigated the relevance of these effects for a SM-like Higgs boson with a mass of 125 GeV and provide a prediction of the corresponding gluon-fusion cross section at the LHC with a center-of-mass energy of 13 TeV. Both for CP-even and -odd Higgs bosons, `SusHi` now calculates the renormalization-scale uncertainty simultaneously to the calculation of the gluon-fusion cross section at the central scale. Moreover, the effects of dimension-5 operators can be studied in any model currently supported by `SusHi`. We showed how the degeneracy between the top-quark mass contribution and a point-like dimension-5 operator contribution can be broken at large values of the transverse momentum of a Higgs boson with mass 125 GeV. The implementation of arbitrary dimension-5 operators is also particularly suited for the study of new CP-even and -odd scalars beyond the implemented models. We showed the convergence of the perturbative series for the inclusive gluon-fusion cross section of a scalar with mass 750 GeV at the 13 TeV LHC.

Our description includes examples how the user can control the new features through the setting of blocks in the input file of `SusHi`. Example input files are contained in the `/example` folder of the current `SusHi` release to be found at [8].

Acknowledgments

RVH would like to thank DFG for financial support. SL acknowledges support by the SFB 676 "Particles, Strings and the Early Universe".

References

[1] G. Aad *et al.* [ATLAS Collaboration], Phys. Lett. B **716** (2012) 1 [arXiv:1207.7214].
[2] S. Chatrchyan *et al.* [CMS Collaboration], Phys. Lett. B **716** (2012) 30 [arXiv:1207.7235].
[3] S. Dittmaier *et al.* [LHC Higgs Cross Section Working Group Collaboration], "Handbook of LHC Higgs Cross Sections: 1. Inclusive Observables," arXiv:1101.0593.
[4] S. Dittmaier *et al.* [LHC Higgs Cross Section Working Group Collaboration], "Handbook of LHC Higgs Cross Sections: 2. Differential Distributions," arXiv:1201.3084.
[5] S. Heinemeyer *et al.* [LHC Higgs Cross Section Working Group Collaboration], "Handbook of LHC Higgs Cross Sections: 3. Higgs Properties," arXiv:1307.1347.
[6] Fourth edition of the "Handbook of LHC Higgs Cross Sections", to be released.
[7] R. V. Harlander, S. Liebler and H. Mantler, Comput. Phys. Commun. **184** (2013) 1605 [arXiv:1212.3249].
[8] Webpage of `SusHi`: http://sushi.hepforge.org.
[9] S. Liebler, Eur. Phys. J. C **75** (2015) 5, 210 [arXiv:1502.07972].

[10] M. Spira, hep-ph/9510347.
[11] E. Bagnaschi, G. Degrassi, P. Slavich and A. Vicini, JHEP **1202** (2012) 088 [arXiv:1111.2854].
[12] C. Anastasiou, S. Buehler, F. Herzog and A. Lazopoulos, JHEP **1112** (2011) 058 [arXiv:1107.0683].
[13] C. Anastasiou, S. Bucherer and Z. Kunszt, JHEP **0910** (2009) 068 [arXiv:0907.2362].
[14] S. Catani and M. Grazzini, Phys. Rev. Lett. **98** (2007) 222002 [hep-ph/0703012].
[15] S. Catani and M. Grazzini, PoS RADCOR **2007** (2007) 046 [arXiv:0802.1410].
[16] R. D. Ball, M. Bonvini, S. Forte, S. Marzani and G. Ridolfi, Nucl. Phys. B **874** (2013) 746 [arXiv:1303.3590].
[17] M. Bonvini, R. D. Ball, S. Forte, S. Marzani and G. Ridolfi, J. Phys. G **41** (2014) 095002 [arXiv:1404.3204].
[18] M. Bonvini, S. Marzani, C. Muselli and L. Rottoli, arXiv:1603.08000.
[19] C. Anastasiou, C. Duhr, F. Dulat, E. Furlan, T. Gehrmann, F. Herzog and B. Mistlberger, JHEP **1503** (2015) 091 [arXiv:1411.3584].
[20] C. Anastasiou, C. Duhr, F. Dulat, F. Herzog and B. Mistlberger, Phys. Rev. Lett. **114** (2015) 212001 [arXiv:1503.06056].
[21] C. Anastasiou, C. Duhr, F. Dulat, E. Furlan, F. Herzog and B. Mistlberger, JHEP **1508** (2015) 051 [arXiv:1505.04110].
[22] C. Anastasiou, C. Duhr, F. Dulat, E. Furlan, T. Gehrmann, F. Herzog, A. Lazopoulos and B. Mistlberger, arXiv:1602.00695.
[23] S. Marzani, R. D. Ball, V. Del Duca, S. Forte and A. Vicini, Nucl. Phys. B **800** (2008) 127 [arXiv:0801.2544].
[24] R. V. Harlander, H. Mantler, S. Marzani and K. J. Ozeren, Eur. Phys. J. C **66** (2010) 359 [arXiv:0912.2104].
[25] R. V. Harlander and K. J. Ozeren, JHEP **0911** (2009) 088 [arXiv:0909.3420].
[26] R. V. Harlander and K. J. Ozeren, Phys. Lett. B **679** (2009) 467 [arXiv:0907.2997].
[27] A. Pak, M. Rogal and M. Steinhauser, JHEP **1002** (2010) 025 [arXiv:0911.4662].
[28] A. Pak, M. Rogal and M. Steinhauser, Phys. Lett. B **679** (2009) 473 [arXiv:0907.2998].
[29] A. Pak, M. Rogal and M. Steinhauser, JHEP **1109** (2011) 088 [arXiv:1107.3391].
[30] R. V. Harlander, Eur. Phys. J. C **76** (2016) 252 [arXiv:1512.04901].
[31] H. M. Georgi, S. L. Glashow, M. E. Machacek and D. V. Nanopoulos, Phys. Rev. Lett. **40** (1978) 692.
[32] A. Djouadi, M. Spira and P. M. Zerwas, Phys. Lett. B **264** (1991) 440.
[33] S. Dawson, Nucl. Phys. B **359** (1991) 283.
[34] M. Spira, A. Djouadi, D. Graudenz and P. M. Zerwas, Nucl. Phys. B **453** (1995) 17 [hep-ph/9504378].
[35] R. Harlander and P. Kant, JHEP **0512** (2005) 015 [hep-ph/0509189].
[36] C. Anastasiou, S. Beerli, S. Bucherer, A. Daleo and Z. Kunszt, JHEP **0701** (2007) 082 [hep-ph/0611236].
[37] U. Aglietti, R. Bonciani, G. Degrassi and A. Vicini, JHEP **0701** (2007) 021 [hep-ph/0611266].
[38] R. V. Harlander and W. B. Kilgore, Phys. Rev. Lett. **88** (2002) 201801 [hep-ph/0201206].
[39] C. Anastasiou and K. Melnikov, Nucl. Phys. B **646** (2002) 220 [hep-ph/0207004].
[40] V. Ravindran, J. Smith and W. L. van Neerven, Nucl. Phys. B **665** (2003) 325 [hep-ph/0302135].
[41] C. Anastasiou, C. Duhr, F. Dulat, E. Furlan, T. Gehrmann, F. Herzog and B. Mistlberger, Phys. Lett. B **737** (2014) 325 [arXiv:1403.4616].
[42] Y. Li, A. von Manteuffel, R. M. Schabinger and H. X. Zhu, Phys. Rev. D **91** (2015) 036008 [arXiv:1412.2771].
[43] M. Höschele, J. Hoff, A. Pak, M. Steinhauser and T. Ueda, Phys. Lett. B **721** (2013) 244 [arXiv:1211.6559].
[44] P. A. Baikov, K. G. Chetyrkin, A. V. Smirnov, V. A. Smirnov and M. Steinhauser, Phys. Rev. Lett. **102** (2009) 212002 [arXiv:0902.3519].
[45] R. N. Lee, A. V. Smirnov and V. A. Smirnov, JHEP **1004** (2010) 020 [arXiv:1001.2887].
[46] T. Gehrmann, E. W. N. Glover, T. Huber, N. Ikizlerli and C. Studerus, JHEP **1006** (2010) 094 [arXiv:1004.3653].

[47] T. Gehrmann, E. W. N. Glover, T. Huber, N. Ikizlerli and C. Studerus, JHEP **1011** (2010) 102 [arXiv:1010.4478].
[48] T. Gehrmann, M. Jaquier, E. W. N. Glover and A. Koukoutsakis, JHEP **1202** (2012) 056 [arXiv:1112.3554].
[49] W. B. Kilgore, Phys. Rev. D **89** (2014) 073008 [arXiv:1312.1296].
[50] C. Duhr, T. Gehrmann and M. Jaquier, JHEP **1502** (2015) 077 [arXiv:1411.3587].
[51] C. Duhr and T. Gehrmann, Phys. Lett. B **727** (2013) 452 [arXiv:1309.4393].
[52] C. Anastasiou, C. Duhr, F. Dulat and B. Mistlberger, JHEP **1307** (2013) 003 [arXiv:1302.4379].
[53] M. Höschele, J. Hoff and T. Ueda, JHEP **1409** (2014) 116 [arXiv:1407.4049].
[54] F. Dulat and B. Mistlberger, arXiv:1411.3586.
[55] C. Anzai, A. Hasselhuhn, M. Höschele, J. Hoff, W. Kilgore, M. Steinhauser and T. Ueda, JHEP **1507** (2015) 140 [arXiv:1506.02674].
[56] Y. Li, A. von Manteuffel, R. M. Schabinger and H. X. Zhu, Phys. Rev. D **90** (2014) 053006 [arXiv:1404.5839].
[57] D. de Florian, J. Mazzitelli, S. Moch and A. Vogt, JHEP **1410** (2014) 176 [arXiv:1408.6277].
[58] S. Actis, G. Passarino, C. Sturm and S. Uccirati, Phys. Lett. B **670** (2008) 12 [arXiv:0809.1301].
[59] U. Aglietti, R. Bonciani, G. Degrassi and A. Vicini, Phys. Lett. B **595** (2004) 432 [hep-ph/0404071].
[60] R. Bonciani, G. Degrassi and A. Vicini, Comput. Phys. Commun. **182** (2011) 1253 [arXiv:1007.1891].
[61] S. Catani, D. de Florian, M. Grazzini and P. Nason, JHEP **0307** (2003) 028 [hep-ph/0306211].
[62] S. Moch and A. Vogt, Phys. Lett. B **631** (2005) 48 [hep-ph/0508265].
[63] A. Idilbi, X. d. Ji, J. P. Ma and F. Yuan, Phys. Rev. D **73** (2006) 077501 [hep-ph/0509294].
[64] A. Idilbi, X. d. Ji and F. Yuan, Nucl. Phys. B **753** (2006) 42 [hep-ph/0605068].
[65] V. Ravindran, Nucl. Phys. B **752** (2006) 173 [hep-ph/0603041].
[66] V. Ahrens, T. Becher, M. Neubert and L. L. Yang, Eur. Phys. J. C **62** (2009) 333 [arXiv:0809.4283].
[67] T. Schmidt and M. Spira, Phys. Rev. D **93** (2016) 014022 [arXiv:1509.00195].
[68] G. Degrassi and P. Slavich, JHEP **1011** (2010) 044 [arXiv:1007.3465].
[69] G. Degrassi, S. Di Vita and P. Slavich, JHEP **1108** (2011) 128 [arXiv:1107.0914].
[70] G. Degrassi, S. Di Vita and P. Slavich, Eur. Phys. J. C **72** (2012) 2032 [arXiv:1204.1016].
[71] R. V. Harlander and M. Steinhauser, Phys. Lett. B **574** (2003) 258 [hep-ph/0307346].
[72] R. V. Harlander and M. Steinhauser, JHEP **0409** (2004) 066 [hep-ph/0409010].
[73] R. V. Harlander and F. Hofmann, JHEP **0603** (2006) 050 [hep-ph/0507041].
[74] G. Degrassi and P. Slavich, Nucl. Phys. B **805** (2008) 267 [arXiv:0806.1495].
[75] A. Pak, M. Steinhauser and N. Zerf, Eur. Phys. J. C **71** (2011) 1602 [Eur. Phys. J. C **72** (2012) 2182] [arXiv:1012.0639].
[76] A. Pak, M. Steinhauser and N. Zerf, JHEP **1209** (2012) 118 [arXiv:1208.1588].
[77] R. Harlander and M. Steinhauser, Phys. Rev. D **68** (2003) 111701 [hep-ph/0308210].
[78] E. Bagnaschi, R. V. Harlander, S. Liebler, H. Mantler, P. Slavich and A. Vicini, JHEP **1406** (2014) 167 [arXiv:1404.0327].
[79] C. Anastasiou, S. Beerli and A. Daleo, Phys. Rev. Lett. **100** (2008) 241806 [arXiv:0803.3065].
[80] M. Mühlleitner, H. Rzehak and M. Spira, PoS RADCOR **2009** (2010) 043 [arXiv:1001.3214].
[81] M. Mühlleitner and M. Spira, Nucl. Phys. B **790** (2008) 1 [hep-ph/0612254].
[82] F. Maltoni, Z. Sullivan and S. Willenbrock, Phys. Rev. D **67** (2003) 093005 [hep-ph/0301033].
[83] R. V. Harlander and W. B. Kilgore, Phys. Rev. D **68** (2003) 013001 [hep-ph/0304035].
[84] S. Heinemeyer, W. Hollik and G. Weiglein, Comput. Phys. Commun. **124** (2000) 76 [hep-ph/9812320].
[85] S. Heinemeyer, W. Hollik and G. Weiglein, Eur. Phys. J. C **9** (1999) 343 [hep-ph/9812472].
[86] G. Degrassi, S. Heinemeyer, W. Hollik, P. Slavich and G. Weiglein, Eur. Phys. J. C **28** (2003) 133 [hep-ph/0212020].
[87] M. Frank, T. Hahn, S. Heinemeyer, W. Hollik, H. Rzehak and G. Weiglein, JHEP **0702** (2007) 047 [hep-ph/0611326].
[88] D. Eriksson, J. Rathsman and O. Stål, Comput. Phys. Commun. **181** (2010) 189 [arXiv:0902.0851].
[89] P. Z. Skands *et al.*, JHEP **0407** (2004) 036 [hep-ph/0311123].

[90] C. Anastasiou, R. Boughezal and F. Petriello, JHEP **0904** (2009) 003 [arXiv:0811.3458].
[91] M. Höschele, J. Hoff, A. Pak, M. Steinhauser and T. Ueda, Comput. Phys. Commun. **185** (2014) 528 [arXiv:1307.6925].
[92] D. Graudenz, M. Spira and P. M. Zerwas, Phys. Rev. Lett. **70** (1993) 1372.
[93] K. A. Olive *et al.* [Particle Data Group Collaboration], Chin. Phys. C **38** (2014) 090001.
[94] S. Marzani, PhD thesis 2008, University of Edinburgh, [http://hdl.handle.net/1842/3156].
[95] R. J. Crewther, Phys. Rev. Lett. **28** (1972) 1421.
[96] M. S. Chanowitz and J. R. Ellis, Phys. Lett. B **40** (1972) 397.
[97] M. S. Chanowitz and J. R. Ellis, Phys. Rev. D **7** (1973) 2490.
[98] J. C. Collins, A. Duncan and S. D. Joglekar, Phys. Rev. D **16** (1977) 438.
[99] C. Grojean, E. Salvioni, M. Schlaffer and A. Weiler, JHEP **1405** (2014) 022 [arXiv:1312.3317].
[100] J. Butterworth *et al.*, J. Phys. G **43** (2016) 023001 [arXiv:1510.03865].
[101] S. Dulat *et al.*, Phys. Rev. D **93** (2016) 033006 [arXiv:1506.07443].
[102] L. A. Harland-Lang, A. D. Martin, P. Motylinski and R. S. Thorne, Eur. Phys. J. C **75** (2015) 204 [arXiv:1412.3989].
[103] R. D. Ball *et al.* [NNPDF Collaboration], JHEP **1504** (2015) 040 [arXiv:1410.8849].
[104] J. Gao and P. Nadolsky, JHEP **1407** (2014) 035 [arXiv:1401.0013].
[105] S. Carrazza, S. Forte, Z. Kassabov, J. I. Latorre and J. Rojo, Eur. Phys. J. C **75** (2015) 369 [arXiv:1505.06736].
[106] S. Carrazza, J. I. Latorre, J. Rojo and G. Watt, Eur. Phys. J. C **75** (2015) 474 [arXiv:1504.06469].
[107] A. Denner *et al.*, LHCHXSWG-INT-2015-006.
[108] M. Cacciari and N. Houdeau, JHEP **1109** (2011) 039 [arXiv:1105.5152].
[109] CMS Collaboration, CMS-PAS-EXO-16-018.
[110] ATLAS Collaboration, ATLAS-CONF-2016-018.